PASSIVE TREATMENT OF ACID ROCK DRAINAGE: TREATMENT SYSTEM LIMITATIONS AND LABORATORY COMPARISON OF SILICATE REACTIVE SUBSTRATES

A Thesis
Presented in Partial Fulfillment of the Requirements for the
Degree of Master of Science
with a
Major in Geology
in the
College of Graduate Studies
University of Idaho
by

Wes R. Sandlin

Major Professor: Jeff Langman, Ph.D.
Committee Members: James Moberly, Ph.D.; Kristopher Waynant, Ph.D.
Department Administrator: Leslie Baker, Ph.D.

May 2020

AUTHORIZATION TO SUBMIT THESIS

This thesis of Wes R. Sandlin, submitted for the degree of Master of Science with a Major in Geology and titled "Passive Treatment of Acid Rock Drainage: Treatment System Limitations and Laboratory Comparison of Silicate Reactive Substrates," has been reviewed in final form. Permission, as indicated by the signatures and dates below, is now granted to submit final copies to the College of Graduate Studies for approval.

Major Professor: _____ Date: _____
Jeff Langman, Ph.D.

Committee Members: _____ Date: _____
James Moberly, Ph.D.

_____ Date: _____
Kristopher Waynant, Ph.D.

Department Administrator: _____ Date: _____
Leslie Baker, Ph.D.

ABSTRACT

The generation of acid rock drainage (ARD) continues to significantly impact water resources around the globe. Passive treatment systems have been developed as lower-cost remediation alternatives to active treatment systems, but seasonality of flow, acidity, and metal concentrations present challenges for passive systems. This thesis examines the limitations of current passive treatment system options and explores the potential of a manufactured silica fiber functionalized with (3-Aminopropyl)triethoxysilane (Si+APTES) and a naturally occurring silicate mineral (clinoptilolite) as reactive substrates for passive treatment of ARD.

The first chapter is a review of passive treatment options for acid rock drainage. This review indicates reduced efficacy due to seasonal periods of increased drainage and metal concentrations that lead to mineral precipitation, surface passivation, and flow bypass. In select cases, passive treatment systems prematurely failed due to seasonal flux. Complimentary systems are needed to minimize impacts from seasonal flux of drainage and metal concentrations to improve treatment efficacy and preserve the life of a multi-component system or a downstream primary system. Multi-component systems are possible with integration of existing treatment systems and design of new treatment options to tailor treatment to site specifications.

The second chapter explores Si+APTES and clinoptilolite as potential reactive substrates for passive treatment of acid rock drainage. Column permeability experiments with silica fiber and loosely packed clinoptilolite indicate greater permeability and stability of the clinoptilolite. Batch sorption experiments with bare silica fiber, Si+APTES, and clinoptilolite in an Fe-SO_4, pH 3.0 solution indicate an Fe specific sorption efficacy of Si+APTES > clinoptilolite > bare silica fiber at equivalent surface areas. Specific sorption values normalized to possible packing densities indicate greater sorption per volume for clinoptilolite. Sorption results for Si+APTES and clinoptilolite did not produce isotherms that could be described by the Langmuir or Freundlich models likely because of surface heterogeneity and precipitation reactions. Column sorption experiments under flowing conditions indicate an Fe removal efficacy of clinoptilolite > Si+APTES for permeable packing densities. Si+APTES demonstrated high specific sorption of Fe in batch sorption experiments and has potential use in low-flow, passive treatment of acid rock drainage. The balance of greater permeability, stability under flowing conditions, large surface area, microporous structure, and ion-exchange properties of clinoptilolite make these zeolite grains a better reactive substrate for passive treatment of acidic drainage in high- or low-flow conditions.

ACKNOWLEDGEMENTS

I would like to thank the members of my committee for their guidance and expertise during my time at the University of Idaho. Dr. Jeff Langman has been a mentor to me, pushing me to grow and improve as a scientist and preparing me for a career after graduation. I thank Dr. James Moberly for his time, generosity, and perspective, which aided our research immensely. I thank Dr. Kristopher Waynant for his advice and assistance in editing manuscripts. Thanks to Thomas Thuneman and Mike Traver-Greene for their massive help in conducting field and lab work. Finally, I thank the faculty and staff of the Department of Geological Sciences at the University of Idaho for a supportive and challenging graduate experience.

This research was supported by the Office of Surface Mining, Reclamation, and Enforcement Applied Science Program, Cooperative Grant Agreement #S17AC20000. Additional funding was provided by the Geological Society of America Graduate Student Research Grant program.

DEDICATION

This thesis is dedicated to my family. My parents, Troy and Dee, have been a constant source of encouragement, belief, and selfless love. I can never thank them enough for the example that they have set for me. I would not be the person that I am today without my incredible siblings Colin and Kylie. I am grateful from the cards, phone calls, and visits from Ilse and Jim Holderby throughout graduate school. To my friends in Birmingham, thank you for staying connected and making Alabama feel close. To my friends in Moscow, thank you for providing me with a new home. Lastly, I would like to thank my wonderful wife, Britne, for her positivity, love, support, understanding, and so much more. I could not have done this without you.

TABLE OF CONTENTS

LIST OF TABLES

LIST OF FIGURES

STATEMENT OF CONTRIBUTION

Coauthors for the works included in this thesis are Jeff Langman, James Moberly, Kristopher Wynant, Mausumi Mukhopadhyay, and Thomas Thuneman. The conceptualization for this project was envisioned by my graduate advisors, Jeff Langman and James Moberly. Methodology for completed work was a combined effort by Wes Sandlin, Jeff Langman, James Moberly, Mausumi Mukhopadhyay, and Kristopher Waynant. All experimentation, formal analysis, modeling, and data visualization was completed by Wes Sandlin. Additional assistance in conducting laboratory and field experiments was provided by Thomas Thuneman. Original drafts of the works included in this thesis were prepared by Wes Sandlin and Jeff Langman, and review and editing were completed as a joint effort by Wes Sandlin, Jeff Langman, James Moberly, Kristopher Waynant, and Mausumi Mukhopadhyay. Primary funding for the completion of the project was acquired by Jeff Langman and James Moberly. Additional funding for the project was acquired by Wes Sandlin.

CHAPTER 1: A REVIEW OF ACID ROCK DRAINAGE, SEASONAL FLUX OF DISCHARGE AND METAL CONCENTRATIONS, AND PASSIVE TREATMENT SYSTEM LIMITATIONS

This is a modified version of an Accepted Manuscript published by Taylor & Francis:

W.R. Sandlin, J.B. Langman, J.G. Moberly, *A review of acid rock drainage, seasonal flux of discharge and metal concentrations, and passive treatment system limitations*, Int. J. Min. Reclam. Env. (2020). pp. 1-14. doi:10.1080/17480930.2020.1728035.

Introduction

The generation of acid rock drainage (ARD) from the weathering of sulfidic ores and waste rock and acidification of resulting drainage continues to significantly impact local and regional water resources across the United States and around the globe [1–4]. Abandoned mine sites with degrading infrastructure, unregulated mine water build-up, and discharge of ARD are acutely difficult sites for remediation. Common methods to address abandoned mine ARD are the reduction of potential discharge through mine dewatering (source control) or downstream collection of the ARD for active or passive treatment [5,6]. Active and passive treatment systems primarily target acidity reduction and associated metal mobility through chemical alteration. Active treatment systems can adjust to changing influent conditions; typically require power, equipment, personnel, and maintenance to continually treat the drainage; and generally have higher operational costs compared to passive methods [3,6]. Passive systems rely on natural physical, chemical, and biological processes to passively treat the drainage without regular maintenance, power inputs, and personnel requirements and typically have lower costs of installation and operation [6–9]. An ARD passive treatment system may be designed for a range of flow rates and metal concentrations, but large pulses of drainage and metals may induce higher rates of mineral precipitation and passivation of reactive surfaces, which can result in clogging or bypass of the treatment components [2,9–12]. Substantial surface passivation and bypass will reduce treatment efficacy (ability to obtain treatment goals) and(or) shorten the life of the treatment system [11,13].

ARD site characteristics, including mineralogy, geomorphology, and biology each influence the weathering of sulfide minerals and the transport of oxidation products; but the hydrology of a site most directly affects the production of ARD through saturation of the weathering mineral surfaces

with oxygenated water and flushing of solutes [14,15]. Design and construction of passive treatment systems can be challenging for sites that experience periods of intense or extended rainfall and(or) snowmelt due to the associated large seasonal flux (temporal variability) of discharge and metal concentrations [2–4,14,16–19]. Strong seasonal differences can make it difficult to estimate representative discharges or metal concentrations, leading to incorrect design of the primary treatment system [20]. Under or over design of the system can shorten the lifespan or significantly increase remediation costs [20].

The inability of passive treatment systems to adjust to changes in discharge and metal concentrations can limit their application in comparison to active treatment systems [6]. Instead of directing all effort to design a singular system for passive treatment of ARD, remediation managers are examining multi-component or modular systems that can provide complimentary treatment or support to a primary passive treatment system [6,20,21]. Flexibility of design, particularly a modular design that allows for refreshing of a treatment component during low volume periods, can reduce the impact of seasonal flux of discharge and metal concentrations, increase treatment efficacy, extend overall system life, decrease costs, and minimize ARD environmental impacts. Following is a review of common passive treatment systems and associated weaknesses, which can be overcome with integration of existing and new passive treatment systems as complimentary modules for ARD remediation. Multi-component passive treatment systems have the potential to improve treatment efficacy and sustain predicted life of the treatment system.

Current passive treatment methods

The challenge of treating ARD has inspired the development of multiple treatment methods divided between active and passive treatment systems [6,9,22,23]. The high cost of active treatment systems led to the rise of passive treatment systems to reduce implementation and maintenance costs along with manpower requirements to sustain treatment [6,22]. The four primary ARD passive treatment systems—permeable reactive barriers, alkalinity-producing systems, phytoremediation, and bioremediation—each have strengths and weaknesses for deployment in a variety of terrains and environmental conditions, and each system has potential issues in treating the seasonal flux of discharge and metal concentrations of ARD.

Permeable reactive barrier

Permeable reactive barriers (PRBs) are increasingly popular in ARD remediation because of their low cost and low maintenance, but their use is typically limited to sites containing shallow, spatially-limited groundwater plumes of ARD [24–27]. PRBs (Figure 1.1) are composed of porous

reactive materials buried in a trench that intercept contaminated groundwater and capture or degrade the contaminant to an environmentally appropriate form(s) [27–31]. Reactive materials in PRBs vary depending on site characteristics including hydraulic gradient, acidity, and metal concentrations [27–31]. The selected reactive material(s) must be contained within an appropriate trench configuration of sufficient volume and length to ensure the necessary residence time for reducing acidity and metal concentrations, while maintaining permeability and reactivity [28,29,32,33]. PRBs are designed for long-term deployment because of the below ground nature of the treatment system, and a reduction in predicted system life can be a substantial cost if exhumation and modification become necessary [20,26].

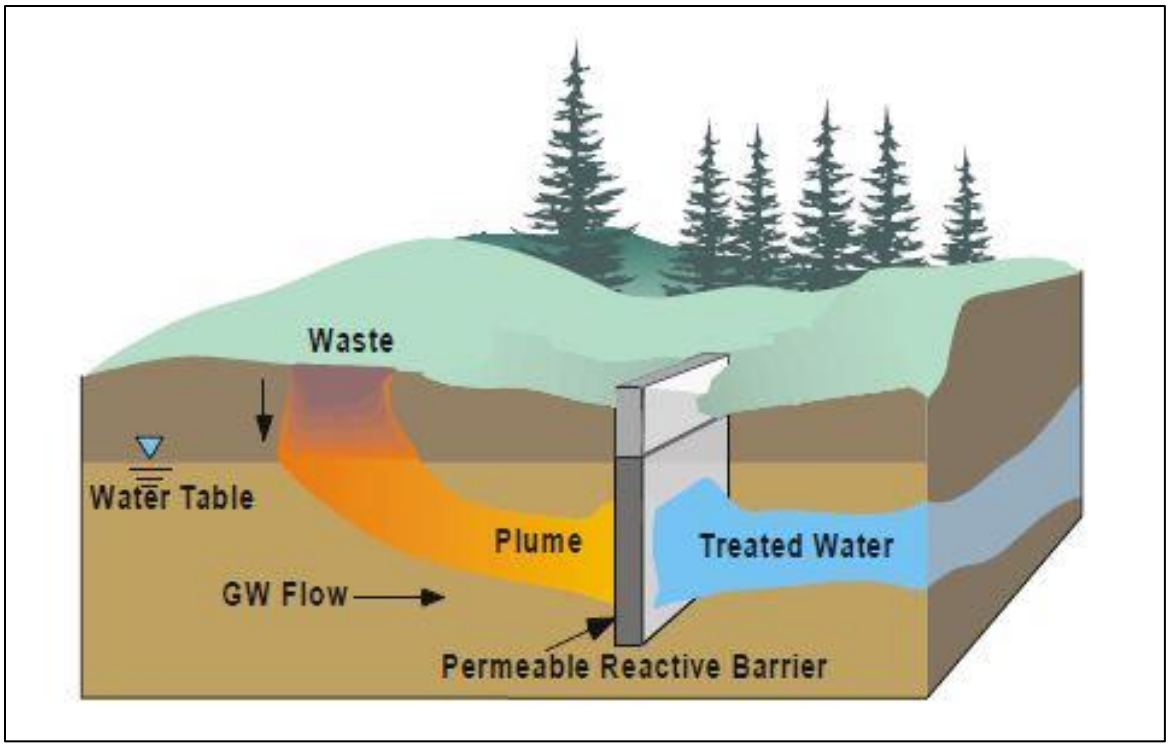

Figure 1.1. Treatment of a contaminant plume by permeable reactive barrier. Courtesy of the EPA [27].

PRB materials may include one or more reactive mediums, such as a reductant (e.g., zero-valent iron (ZVI), large surface area materials for sorption and mineral precipitation (e.g., zeolites, activated carbon, biochar), alkaline materials to reduce acidity (e.g., limestone), and organic materials (e.g., mulch) to enhance biological activity for sulfate (SO_4)-reduction [8,11,27,30,34–37].

PRBs for ARD remediation typically include a mixture of ZVI, organic, and alkaline materials to create suitable conditions for bacterially mediated SO_4-reduction and precipitation of metal sulfides [9,24,28]. Biochar, a substance formed from the pyrolysis of organic material such as agriculture or forestry waste, has become increasingly popular as a reactive material in PRBs because of high sorption capacity and ability to consume acid [16,38–43].

The efficacy of a PRB depends on the reactivity and availability of the materials and sustained permeability for sufficient residence time in this below ground system [33,34]. Thorough hydrogeologic and geochemical assessments of the contaminated site are necessary prior to the design and implementation of a PRB [27,44]. Unanticipated ARD seasonal flux in drainage and metal concentrations can result in reduced reactivity (surface passivation), clogging, and flow bypass [32]. Use of reactive material with large grain sizes can sustain greater permeability and reduce preferential flow but also reduces available reactive surface area [24,28,29]. Smaller grain sizes allow longer residence time but are more prone to preferential flow as precipitates clog pore-spaces [24,28,29]. Limited plume capture or system bypass can occur if the permeability of the PRB is reduced with mineral precipitation and clogging [24,26,32,44]. Balancing permeability, residence time, and reactive surface contact is crucial to the efficacy of a PRB [10,11,26,28,29,32,33,44].

Alkalinity-producing systems

Alkalinity-producing systems are passive systems that use calcium oxide (CaO), calcium carbonate ($CaCO_3$), sodium carbonate (NaCO3), sodium hydroxide (NaOH), or natural lime (calcium-containing inorganic materials of carbonate, hydroxide, and oxide form) to consume acid and precipitate metals that were soluble under acidic conditions [6,9,45,46]. Anoxic limestone drains (ALDs) and open limestone channels (OLCs) (Figure 1.2) are two of the most prominent alkalinity-producing systems, along with less popular limestone leach beds (LLBs) and steel slag leach beds (SLBs) [9,47]. These systems typically have low installation and maintenance costs, but each require specific ARD conditions to ensure high efficacy over the predicted life of the system [9,48].

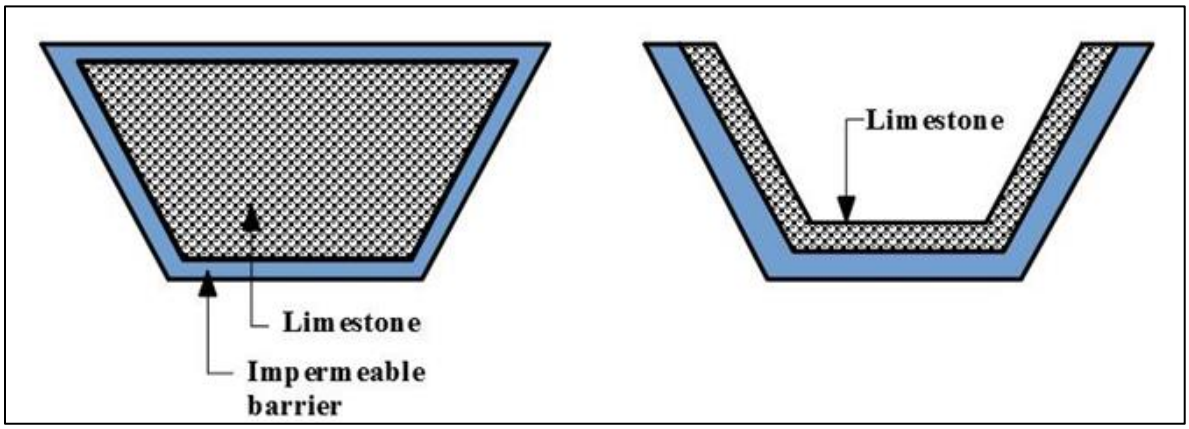

Figure 1.2. Cross-sectional view of anoxic limestone drain (left) and an open limestone channel (right).

ALDs consist of trenches filled with crushed limestone and downgradient settling ponds for retention of precipitating metals [22,49,50]. ALDs typically are covered by clay and(or) a vegetative soil cap to retain CO_2 and exclude O_2 to minimize Fe^{2+} oxidation and Fe-(oxyhydr)oxide precipitation, which would reduce acid neutralization, limit permeability, and shorten the life of the treatment system [6,51,52]. Preventing O_2 entrance into an ALD allows CO_2 to build up within the system– neutralizing acid and allowing for greater metal removal in settling ponds when treated ARD exits the ALD [6,22]. ALDs are best suited for acidic water with low metal concentrations, hypoxic conditions, and limited change in environmental conditions [9,53].

OLCs consist of open channels lined with a layer of limestone and include one or more settling ponds to collect mineral precipitates [9,45,48,50]. The channel is steeply sloped to increase discharge velocity, induce turbulence that scours passivated limestone surfaces, and suspend minerals formed with decreases in acidity [9,45,48,50]. If discharge velocity decreases, precipitates can passivate limestone surfaces and clog channels [45,48,50,54,55]. Effluent drainage from an OLC is directed towards settling ponds where suspended metal forms settle, sorbed to manufactured materials (e.g., high surface area plastics [45]), or are retained by plants through phytoremediation [9,33]. Typically, OLCs can treat ARD with higher metal and dissolved oxygen concentrations compared to ALDs [9].

Less common forms of alkalinity-producing systems include LLBs and SLBs that have limited application in ARD remediation [9,50]. LLBs are open ponds filled with limestone designed to allow for long residence time (e.g., a minimum residence time of 12 hours) necessary to reduce acidity [22,55]. SLBs have a similar design, but contain steel manufacturing waste with high

concentrations of alkalinity-producing minerals such as $Ca(OH)_2$ and (Ca, Fe)-silicates [56,57]. These minerals are formed as a by-product of steel manufacturing due to the addition of limestone or dolomite to the smelting process to assist in the removal of impurities [57,58]. Like ALDs, LLBs and SLBs are designed to interact with ARD containing lower metal concentrations to minimize surface passivation [9]. The need for lower metal concentrations substantially restricts the application of these passive treatment systems, particularly in areas with large seasonal fluxes of ARD [1,3,4].

Phytoremediation

Phytoremediation is a relatively newer passive treatment system for ARD that utilizes acid- and metal-tolerant plants in constructed wetlands (surface ARD) or contaminated soils (surface to shallow subsurface ARD) to remove metals through phytoextraction and phytostabilization (Figure 1.3) [22,59–63]. Phytoextraction involves plants transporting metals from ARD-contaminated soil to their shoots (hyper-accumulator plants) where they are stored and eventually harvested for metal processing or hazardous waste disposal [22,59]. Phytostabilization utilizes root systems to reduce the distribution of a contaminant(s) by inhibiting erosion and adsorbing metals and mineral precipitates to root systems and the surrounding soil matrix [22,59,62,63]. Phytoremediation relies on living organisms that have specific tolerances to acidity, salinity, and other contaminants; therefore, the use of phytoremediation is limited to environments with low metal concentrations that are suitable for plant life and tolerance ranges of specific species [59].

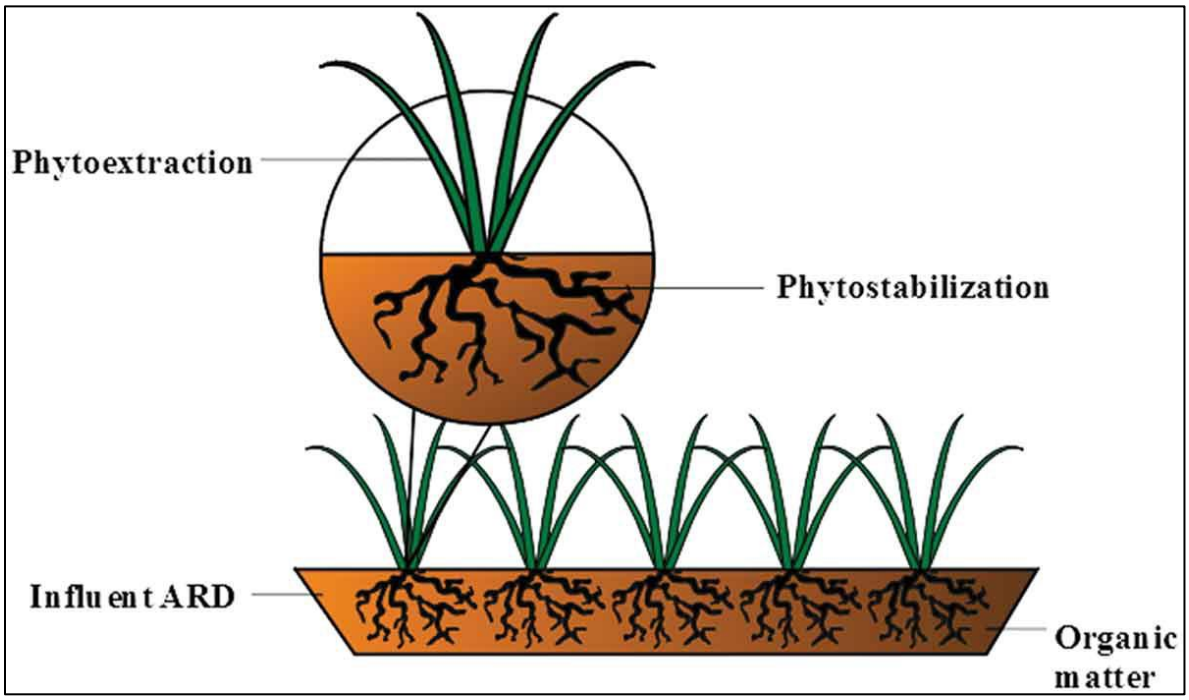

Figure 1.3. Phytoremediation of influent ARD (orange) through phytoextraction and phytostabilization.

At least 400 hyper-accumulator plants have been identified, including bulrush (Scirpus validus), bunchgrass (Vetiveria zizanioides L), cattail (Typha latifolia), and tickseed sunflower (Bidens aristosa) [61,64–66]. Unfortunately, most hyperaccumulator plants grow slowly and cannot produce enough biomass to sufficiently remediate metal-contaminated sites or ARD through phytoextraction alone [59,66]. Phytoremediation studies indicate that phytostabilization is the more effective at reducing metal concentrations in ARD compared to phytoextraction [61,67,68]. Karathanasis and Johnson (2003) suggest that plants for phytoremediation should be selected on metal tolerance and root system surface area rather than bioaccumulation potential. Phytoremediation alone has shown little promise due to the biological and chemical limitations of plants, but the incorporation of metal-tolerant plants with other ARD remediation systems to promote phytostabilization may assist in treatment system efficacy [61,65,68,69].

Bioremediation

Similar to phytoremediation, bioremediation utilizes living organisms to reduce acidity and immobilize metals; however, bioremediation primarily relies on SO_4-reducing bacteria (SRBs) for precipitation of metal-sulfide minerals [6,9,22,32,70]. Bioremediation is often implemented with other forms of passive treatment systems (permeable reactive barriers (PRBs), alkalinity-producing

systems, phytoremediation), or functions as a primary passive treatment system in the form of a passive bioreactor (Figure 1.4) [6,9,22,59,70]. In a passive bioreactor ARD flows through an organic matter matrix, often with a corresponding alkalinity-producing material, to allow for oxidation of organic matter, stimulation of SRB, reduction of acidity, and metal-sulfide precipitation [9,32,70] (Equation 1.1).

$$2CH_2O_{(s)} + SO_4^{2-}{}_{(aq)} + M^{2+} \leftrightarrow MS_{(s)} + 2H_2CO_3 \quad (1.1)$$

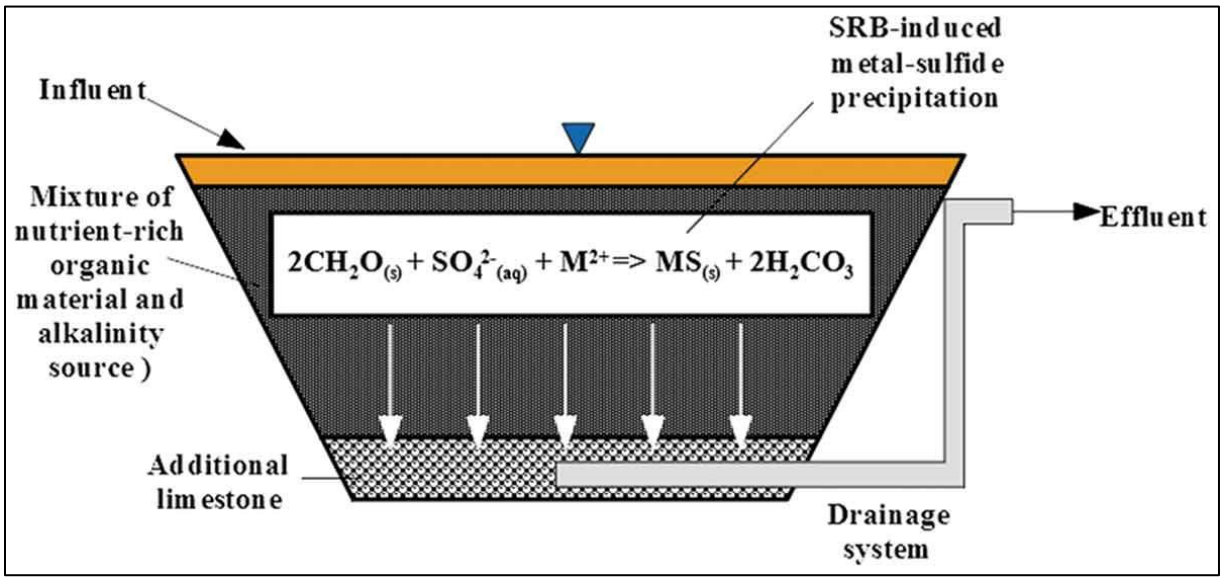

Figure 1.4. Example configuration of a passive bioreactor.

Organic matter such as compost or manure provides nutrients (N, P, and C) that aid in microbial growth to sustain SO_4 reduction [9,32,71]. The addition of an alkalinity source, such as biochar, mussel shells, limestone, or other calcareous wastes, can reduce acidity and allow for greater growth of SRBs, which prefer a more neutral pH environment for optimal sulfate reduction [9,22,32,40,41,72,73]. Metal sulfides produced with bioremediation must remain in an anoxic environment, or their oxidation would release metals back into solution and may produce acid (e.g., Equation 1.2 for an Fe-sulfide) [9]. Bioremediation is often incorporated with other treatment methods such as PRBs and certain alkalinity-producing systems (e.g., ALD) to promote SO_4 reduction, acid neutralization, and mineral precipitation in O_2-free or O_2-limited environments [9].

$$FeS_2 + \frac{7}{2}O_2 + H_2O \leftrightarrow Fe^{2+} + 2SO_4^{2-} + 2H^+ \quad (1.2)$$

Passive bioreactors can accept ARD with high acidity and metal concentrations, but such conditions can be limited by SRB growth [9]. If SRB growth and activity are limited, the efficacy of a bioreactor will be limited and may require a large-scale system where ARD is substantive [9]. High efficacy bioreactors require a neutral, reducing environment with a continuous supply of nutrients and SO_4, as well as an available internal matrix for microbial and metal sorption [22]. These systems need regular refreshment of organic matter and drainage of by-product sludge, which can require active maintenance and(or) limit the predicted life of a purely passive system [9,22]. Furthermore, seasonal flux of discharges and metal concentrations can inhibit SRB growth by introducing oxygen into anoxic zones and increasing metal or acid concentrations, which may destabilize the microbial community and limit the efficacy of bioremediation [2,10–12,55].

Common problems associated with passive treatment systems

The physical, chemical, and biological processes that determine the performance of a passive treatment system are affected by parameters such as acidity, temperature, metal concentrations, and dissolved oxygen [23,29,70,74–77]. Seasonal fluxes in these parameters can result in reduced treatment efficacy, commonly due to the passivation of reactive surfaces or system clogging and bypass [2,9–12]. Additionally, periods of elevated metal, acid, and(or) dissolved oxygen concentrations can disrupt SRB processes crucial to bioremediation [70]. Designing a functional, long-term passive treatment system can be difficult due to the range of parameters that must be considered and the variation of the parameters that a site may experience [23,24,78].

Sorption, mineral precipitation, and surface passivation

Metal sorption and(or) mineral precipitation within a treatment system will reduce surface reactivity and ultimately determine the life of the system [9,20,44,48,54,79,80]. Acid neutralization from the sorption of protons (H^+) to reactive surfaces and the cell walls of microorganisms can also passivate reactive surfaces (protonation), reducing treatment efficacy within a passive treatment system [70]. Sorbed elements/compounds and precipitates can occur in various forms depending on acidity and reduction-oxidation (redox) conditions that influence metal form/species and solubility [50,54,80,81]. As sorbed metals and mineral precipitates reduce reactive surface availability (Figure 1.5), treatment efficacy is reduced unless additional reactive surface is available in the transport pathways [79,80]. In addition to protonating reactive surfaces, periods of elevated acidity can induce the desorption of previously sorbed elements/compounds by proton exchange [70]. The predicted life

of a passive treatment system is based on the exhaustion of all available reactive surfaces, but system life can be difficult to estimate because of seasonal flux of discharge and metal concentrations [9,44]. Substantial changes in ARD characteristics may induce quicker surface passivation and substantially reduce the life of the treatment system [9,44,48].

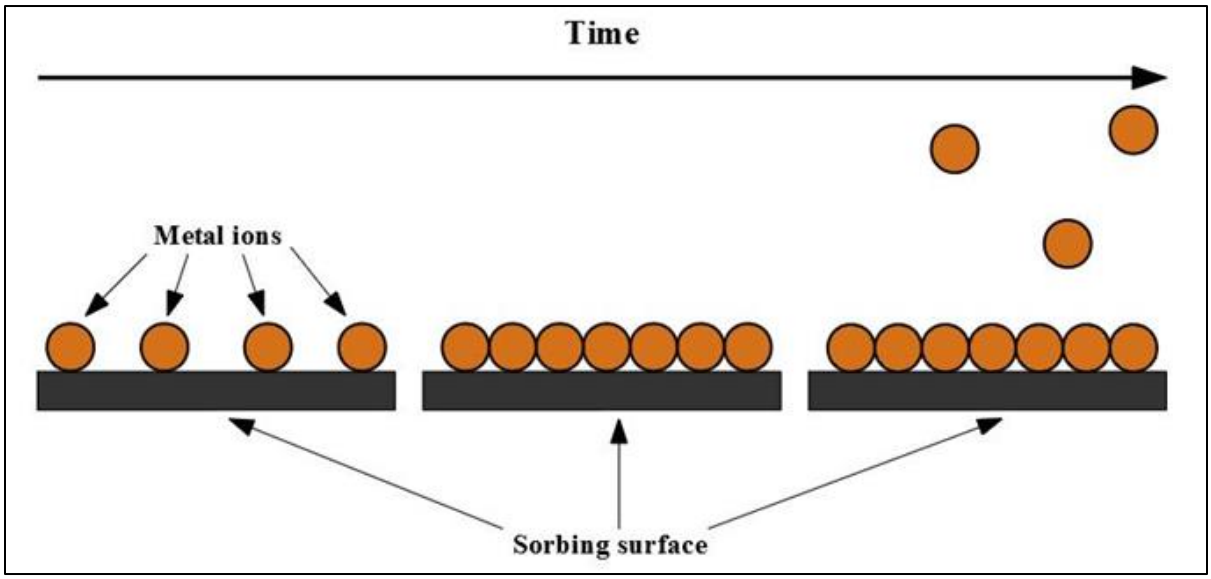

Figure 1.5. Sorption of metal ions on a sorbing surface over time (left to right). The sorbing surface is initially unsaturated; but with time, surface sites are occupied and additional metals either exchange with sorbed metals (no net concentration change) or bypass the sorbing surface.

Precipitation, clogging, and bypass

The accumulation of precipitates or microbial biomass in a passive treatment system has the potential to reduce permeability, clog and alter flowpaths, and reduce residence time (Figure 1.6), which can substantially reduce treatment efficacy [11,20,29,32,81–83]. Bypass is especially problematic in systems such as permeable reactive barriers (PRBs) or anoxic limestone drains (ALDs) where flow is confined and permeability must be sustained to allow for the necessary residence times required for the desired reactions to occur [9,13,29]. Alteration of permeability and development of preferential flowpaths will reduce residence time and lead to further precipitation and surface passivation in the available flowpaths; thereby, initiating a process that can cut off parts of the treatment system from the influent and substantially reduce treatment efficacy [13]. Seasonal flux of

discharge and metal concentrations can increase the rate and severity of this potential problem if the treatment system is not designed to accommodate changes in ARD characteristics [9,10,12,13].

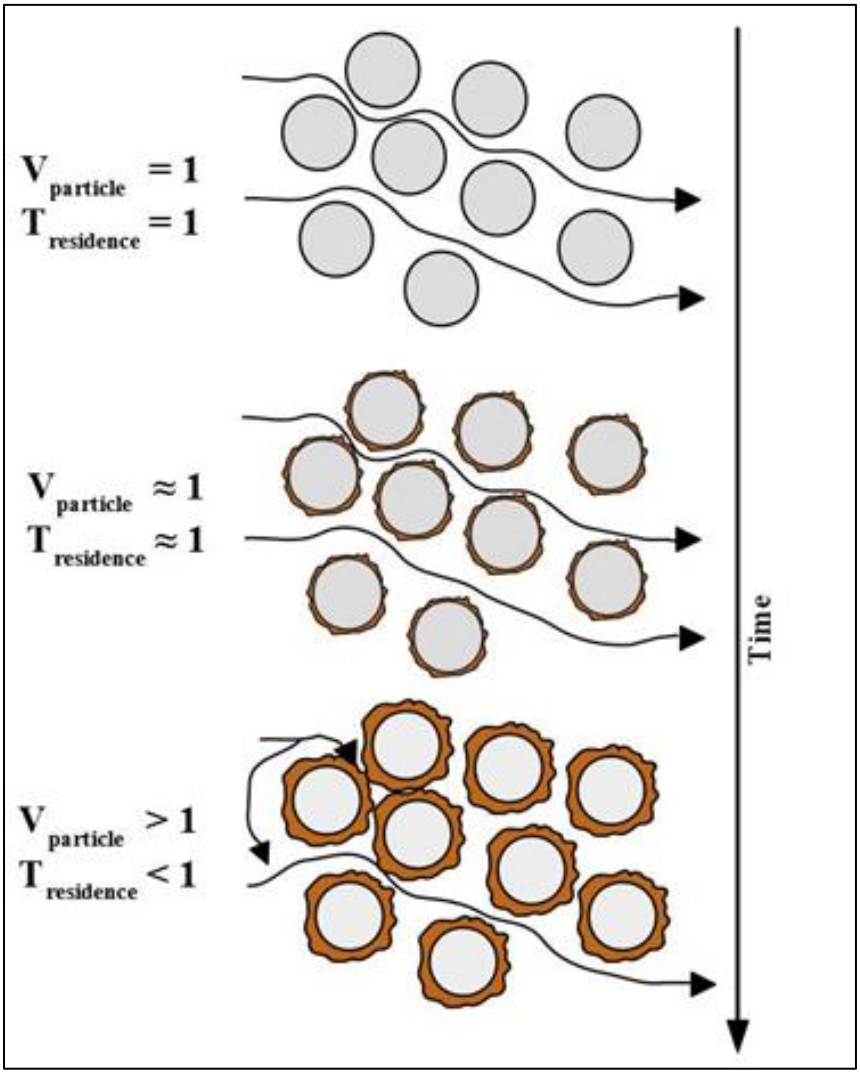

Figure 1.6. Accumulation of precipitates on reactive materials resulting in preferential flow paths and decreased contact times. $\mathbf{V}_{particle}$ = particle velocity; $\boldsymbol{\tau}_{residence}$ = residence time.

Design considerations

The most difficult problem with passive treatment systems is designing and constructing a functioning, lasting system based on an array of physical, hydrological, geochemical, and biological parameters that can be difficult to estimate and(or) maintain [20,23,24,78,84]. Seasonal ARD flux can

induce changes in these parameters; thereby, influencing treatment efficacy, system life, and may require unexpected construction modifications, or reconstruction [2,20,83,84]. The following case studies examine passive treatment systems that experienced seasonal flux of ARD and how their design may have resulted in unsuccessful or successful long-term remediation.

Case study 1: Multi-module permeable reactive barrier

In Aznalcóllar, Spain a PRB was installed to remediate ARD that had impacted the Agrio aquifer. Groundwater had an average pH of 3.4 and high concentrations of SO_4, Zn, Al, and Cu [32,85]. The PRB consisted of three lateral modules filled with various ratios of calcite, vegetable compost, sewage sludge, and zero-valent iron (ZVI) [32,85]. The calcite was included to raise pH and induce metal-(oxy)hydroxide and metal-carbonate precipitation, while organic material and ZVI were included to promote SRB activity and metal-sulfide precipitation [32,85]. Results from downgradient monitoring wells indicated that metal concentrations substantially declined, but SO_4 concentrations were minimally affected [32,85]. It was concluded that metal removal was occurring through (oxy)hydroxide and carbonate precipitation rather than sulfide generation, which potentially contributed to clogging, preferential flow, and bypass of the SRB module [32,85]. Additionally, the PRB system did not fully capture the ARD-impacted groundwater because of under-estimation of ARD flux and contribution to the aquifer [32,85]. The capture issue was magnified during extended periods of heavy rainfall that substantially increased the input of ARD to the aquifer, which expanded the plume beyond the entrance of the PRB [32,85].

Case study 2: Bioremediation + phytoremediation

A passive treatment system consisting of a settling pond and a vegetated bioreactor was installed near Benhar Bing in Glasgow, U.K. to remediate ARD with an average pH of 2.6 and high concentrations of SO_4, Fe, Al, Mg, and Mn [86]. Influent was collected in the settling pond and routed to a bioreactor filled with limestone, mushroom compost, and planted Typhia latifolia (cattail) [86]. The treatment goal was to induce mineral precipitation and SO_4-reduction through SRB and phytostabilizing processes [86]. Evaluation of post-treatment effluent and sediment cores from 6 months of monitoring indicated that SRB activity and limestone dissolution were the primary contributors to contaminant removal, however removal rates for all contaminants did not exceed 30% [86]. The majority of cattail did not survive the low pH influent, and the treatment efficacy of the bioreactor was reduced over time for multiple reasons [86]. Metal ions and mineral precipitates were sorbed by reactive material surfaces within the bioreactor, decreasing the amount of surface area available for the desired reactions to occur [86]. Mineral precipitates clogged pore-spaces, creating

preferential flow and decreasing residence time [86]. Additionally, the majority of sulfide produced by SRB activity was thought to be re-oxidised, resulting in little reduction in SO_4 concentrations [86].

Case study 3: Alkalinity-producing + bioremediation

A passive treatment system in McCreary County, Kentucky, USA, consisting of two consecutive bioreactors, was reconstructed after failing to remediate ARD with a pH range of 2.7 to 4.4 and highly variable SO_4, Al, Fe, and Mn concentrations [87]. In order to improve treatment efficacy, the reconstruction incorporated a multi-module, complimentary passive treatment system design, including alkalinity-producing and bioremediating systems [87]. Influent ARD was collected in an anaerobic pond prior to being routed to an ALD [87]. From the ALD, effluent was directed through five duplicate passive treatment modules, each consisting of a bioreactor and an aerobic settling pond [87]. Evaluation of post-treatment effluent indicated that the combination of anaerobic pond, ALD and repetitive bioreactor/settling pond modules inhibited the surface passivation of ALDs and bioreactors, allowing for substantial reduction in acid, SO_4, and metal concentrations over the 14 months of monitoring [87].

Conclusions

Acid rock drainage (ARD) passive treatment systems can successfully reduce acidity and metal concentrations, but the seasonal flux of ARD can reduce treatment efficacy and(or) reduce system life. Periods of intense precipitation an(or) snowmelt runoff can vary ARD conditions beyond the original design criteria of the passive treatment system. Modification or replacement of improperly designed passive treatment systems can add substantial cost to the remediation project. Permeable reactive barriers, alkalinity-producing systems, phytoremediation, and bioremediation each have potential to reduce the environmental impacts of ARD, but the physical, chemical, and biological processes that determine treatment efficacy for these systems can be affected by seasonal ARD flux and associated problems such as surface passivation and flow bypass. Design integration of complimentary passive treatment types for a multi-component treatment system has shown greater success in remediating ARD compared to individual systems.

If there is potential that the seasonal flux of ARD will impact treatment efficacy and(or) system life of a single type of passive treatment, design of a passive treatment system should focus on integrating complimentary passive treatment types into a multi-component system. In cases of highly variable ARD conditions, multiple treatment types can be integrated to sustain treatment efficacy, either seasonally or continuously, to reduce the burden on one individual system and reduce impacts to the life of the system. Complimentary systems that can assist in reducing acid, metal, dissolved

oxygen, and SO_4 concentrations and variable discharge rates can be spatially integrated with distinct or modular systems in relatively small footprints. A modular design for individual systems would allow additional modules to be incorporated as needed and can provide additional flexibility to assist with construction/deployment as mine drainage evolves. Multi-component passive treatment systems with modular flexibility would be the ideal design to allow for adjustments with seasonal or annual ARD flux to ensure desired drainage conditions and residence time for treatment targets and sustained life of the system.

References

[1] A. Akcil and S. Koldas, *Acid Mine Drainage (AMD): Causes, treatment and case studies*, J Clean. Prod. 14 (2006), pp. 1139–1145. doi:10.1016/j.jclepro.2004.09.006.

[2] R.S. Hedin, R.W. Narin, and R.L. Kleinmann, *Passive Treatment of Coal Mine Drainage*, US Department of the Interior Bureau of Mines, Pittsburgh, PA, 1994.

[3] M.C. Moncur, C.J. Ptacek, M. Hayashi, D.W. Blowes, and S.J. Birks, *Seasonal cycling and mass-loading of dissolved metals and sulfate discharging from an abandoned mine site in northern Canada*, Appl. Geochem. 41 (2014), pp. 176–188. doi:10.1016/j.apgeochem.2013.12.007.

[4] D.K. Nordstrom, *Acid rock drainage and climate change*, J. Geochem. Explor. 100 (2009), pp. 97–104. doi:10.1016/j.gexplo.2008.08.002.

[5] T.J. Hengen, M.K. Squillace, A.D. O'Sullivan, and J.J. Stone, *Life cycle assessment analysis of active and passive acid mine drainage treatment technologies*, Resour. Conserv. Recycl. 86 (2014), pp. 160–167. doi:10.1016/j.resconrec.2014.01.003.

[6] D.B. Johnson and K.B. Hallberg, *Acid mine drainage remediation options: A review*, Sci. Total Environ. 338 (2005), pp. 3–14. doi:10.1016/j.scitotenv.2004.09.002.

[7] N.O. Egiebor and B. Oni, *Acid rock drainage formation and treatment: A review*, Asia-Pac. J. Chem. Eng. 2 (2007), pp. 47–62. doi:10.1002/apj.57.

[8] K.K. Kefeni, T.A.M. Msagati, and B.B. Mamba, *Acid mine drainage: Prevention, treatment options, and resource recovery: A review*, J. Clean. Prod. 151 (2017), pp. 475–493. doi:10.1016/j.jclepro.2017.03.082.

[9] J. Skousen, C.E. Zipper, A. Rose, P.F. Ziemkiewicz, R. Nairn, L.M. McDonald, *Review of passive systems for acid mine drainage treatment*, Mine Water Environ. 36 (2017), pp. 133–153. doi:10.1007/s10230-016-0417-1.

[10] R.D. Ludwig, R.G. McGregor, D.W. Blowes, S.G. Benner, and K. Mountjoy, *A permeable reactive barrier for treatment of heavy metals*, Ground Water 40 (2002), pp. 59–66. doi:10.1111/j.1745-6584.2002.tb02491.x.

[11] P.B. McMahon, K.F. Dennehy, and M.W. Sandstrom, *Hydraulic and geochemical performance of a permeable reactive barrier containing zero-valent iron, Denver Federal Center*, Ground Water 37 (1999), pp. 396–404. doi:10.1111/j.1745-6584.1999.tb01117.x.

[12] R.W. Puls, R.M. Powell, C.J. Paul, and D. Blowes, *Groundwater remediation of chromium using zero-valent iron in a permeable reactive barrier*, in *Innovative Subsurface Remediation*, American Chemical Society, 1999, pp. 182–194. doi:10.1021/bk-1999-0725.ch013.

[13] L. Li, C.H. Benson, and E.M. Lawson, *Impact of mineral fouling on hydraulic behavior of permeable reactive barriers*, Groundwater 43 (2005), pp. 582–596. doi:10.1111/j.1745-6584.2005.0042.x.

[14] E. Gozzard, W.M. Mayes, H.A.B. Potter, and A.P. Jarvis, *Seasonal and spatial variation of diffuse (non-point) source zinc pollution in a historically metal mined river catchment, UK*, Environ. Pollut. 159 (2011), pp. 3113–3122. doi:10.1002/ep.670040311.

[15] D.L. Harris, B.G. Lottermoser, and J. Duchesne, *Ephemeral acid mine drainage at the Montalbion silver mine, north Queensland*, Aust J. Earth Sci. 50 (2003), pp. 797–809. doi:10.1111/j.1440-0952.2003.01029.x.

[16] E.E. August, D.M. McKnight, D.C. Hrncir, and K.S. Garhart, *Seasonal variability of metals transport through a wetland impacted by mine drainage in the Rocky Mountains*, Environ. Sci. Technol. 36 (2002), pp. pp. 3779–3786. doi:10.1021/es015629w.

[17] P. Brooks, D. McKnight, and K. Bencala, *Annual maxima in Zn concentrations during spring snowmelt in streams impacted by mine drainage*, Environ. Geol. 40 (2001), pp. 1447–1454. doi:10.1007/s002540100338.

[18] T.W. Butler, *Isotope geochemistry of drainage from an acid mine impaired watershed, Oakland, California*, Appl. Geochem. 22 (2007), pp. 1416–1426. doi:10.1016/j.apgeochem.2007.01.009.

[19] K.U. Mayer, S.G. Benner, and D.W. Blowes, *Process-based reactive transport modeling of a permeable reactive barrier for the treatment of mine drainage*, J. Contam. Hydrol. 85 (2006), pp. 195–211. doi:10.1016/j.jconhyd.2006.02.006.

[20] C. Costello, *Acid mine drainage: Innovative treatment technologies*, US EPA Office of Solid Waste and Emergency Response Technology Innovation Office, Washington, D.C., 2003.

[21] D.A. Kepler and E.C. McCleary, *Successive alkalinity-producing systems (SAPS) for the treatment of acidic mine drainage*, U.S. Bureau of Mines Special Publication SP 06A. (1994), pp. 195–204. doi:10.21000/JASMR94010195.

[22] A. RoyChowdhury, D. Sarkar, and R. Datta, *Remediation of acid mine drainage-impacted water*, Curr. Pollut. Rep. 1 (2015), pp. 131–141. doi:10.1007/s40726-015-0011-3.

[23] M.S. Ali, *Remediation of acid mine waters*, in *11th International Mine Water Association Congress- Mine Water- Managing the Challenges*, R.T. Rude and A. Freund, eds., Wolkersdorfer, Aachen, 2011, pp. 253–257. ISBN 978-1-897009-47-5.

[24] M.A. Caraballo, E. Santofimia, and A.P. Jarvis, *Metal retention, mineralogy, and design considerations of a mature permeable reactive barrier (PRB) for acidic mine water drainage in Northumberland, U.K.*, Am. Mineral. 95 (2010), pp. 1642–1649. doi:10.2138/am.2010.3505.

[25] A. Johnston, R.L. Runkel, A. Navarre-Sitchler, and K. Singha, *Exploration of diffuse and discrete sources of acid mine drainage to a headwater mountain stream in Colorado, USA*, Mine Water Environ. 36 (2017), pp. 463–478. doi:10.1007/s10230-017-0452-6.

[26] A.N. Shabalala, S.O. Ekolu, and S. Diop, *Permeable reactive barriers for acid mine drainage treatment: A review*, Constr. Mater. Struct. (2014), pp. 1416–1426. doi:10.3233/978-1-61499-466-4-1416.

[27] R.M. Powell, R.W. Puls, D.W. Blowes, J.L. Vogan, R.W. Gillham, P.D. Powell, T. Sivavec, and R. Landis, *Permeable reactive barrier technologies for contaminant remediation*. EPA/600/R-98/125 (NTIS 99-105702), Washington, D.C., 1998.

[28] S.G. Benner, D.W. Blowes, W.D. Gould, R.B. Herbert, and C.J. Ptacek, *Geochemistry of a permeable reactive barrier for metals and acid mine drainage*, Environ. Sci. Technol. 33 (1999), pp. 2793–2799. doi:10.1021/es981040u.

[29] L. Li and C.H. Benson, *Evaluation of five strategies to limit the impact of fouling in permeable reactive barriers*, J. Hazard. Mater. 181 (2010), pp. 170–180. doi:10.1016/j.jhazmat.2010.04.113.

[30] Y. Liu, H. Mou, L. Chen, Z.A. Mirza, and L. Liu, *Cr(VI)-contaminated groundwater remediation with simulated permeable reactive barrier (PRB) filled with natural pyrite as reactive material: Environmental factors and effectiveness*, J. Hazard. Mater. 298 (2015), pp. 83–90. doi:10.1016/j.jhazmat.2015.05.007.

[31] K.R. Waybrant, D.W. Blowes, and C.J. Ptacek, *Selection of reactive mixtures for use in permeable reactive walls for treatment of mine drainage*, Environ. Sci. Technol. 32 (1998), pp. 1972–1979. doi:10.1021/es9703335.

[32] O. Gibert, J.L. Cortina, J. de Pablo, and C. Ayora, *Performance of a field-scale permeable reactive barrier based on organic substrate and zero-valent iron for in situ remediation of acid mine drainage*, Environ. Sci. Pollut. Res. 20 (2013), pp. 7854–7862. doi:10.1007/s11356-013-1507-2.

[33] J.J. Metesh, T. Jarrell, and S. Oravetz, *Treating acid mine drainage from abandoned mines in remote areas*, Tech. Rep. 9871-2821-MTDC, USDA Forest Service, Missoula Technology Development Center, Missoula, MT, 1998.

[34] A.E. Fryar and F.W. Schwartz, *Hydraulic-conductivity reduction, reaction-front propagation, and preferential flow within a model reactive barrier*, J. Contam. Hydrol. 32 (1998), pp. 333–351. doi:10.1016/S0169-7722(98)00057-6.

[35] D.C. McMurtry and R.O. Elton, *New approach to in-situ treatment of contaminated groundwaters*, Environ. Prog. 4 (1985), pp. 168–170. doi:10.1002/ep.670040311.

[36] N. Moraci and P.S. Calabrò, *Heavy metals removal and hydraulic performance in zero-valent iron/pumice permeable reactive barriers*, J. Environ. Manage. 91 (2010), pp. 2336–2341. doi:10.1016/j.jenvman.2010.06.019.

[37] S.J. Morrison and R.R. Spangler, *Chemical barriers for controlling groundwater contamination*, Environ. Prog. 12 (1993), pp. 175–181. doi:10.1002/ep.670120305.

[38] C. Fan and Y. Zhang, *Adsorption isotherms, kinetics and thermodynamics of nitrate and phosphate in binary systems on a novel adsorbent derived from corn stalks*, J. Geochem. Explor. 188 (2018), pp. 95–100. doi:10.1016/j.gexplo.2018.01.020.

[39] M. Holub, M. Balintova, P. Pavlikova, and L. Palascakova, *Study of sorption properties of zeolite in acidic conditions in dependence on particle size*, Ital. Assoc. Chem. Eng. Trans. 32 (2013), pp. 559–564. doi:10.3303/CET1332094.

[40] S. Jain, B.P. Baruah, and P. Khare, *Kinetic leaching of high sulphur mine rejects amended with biochar: Buffering implication*, Ecol. Eng. 71 (2014), pp. 703–709. doi:10.1016/j.ecoleng.2014.08.003.

[41] J. Lehmann, M.C. Rillig, J. Thies, C.A. Masiello, W.C. Hockaday, and D. Crowley, *Biochar effects on soil biota – A review*, Soil Biol. Biochem. 43 (2011), pp. 1812–1836. doi:10.1016/j.soilbio.2011.04.022.

[42] T. Motsi, N.A. Rowson, and M.J.H. Simmons, *Adsorption of heavy metals from acid mine drainage by natural zeolite*, Int. J. Miner. Process. 92 (2009), pp. 42–48. doi:10.1016/j.minpro.2009.02.005.

[43] X. Zhang, H. Wang, L. He, K. Lu, A. Sarmah, J. Li, et al., *Using biochar for remediation of soils contaminated with heavy metals and organic pollutants*, Environ. Sci. Pollut. Res. 20 (2013), pp. 8472–8483. doi:10.1007/s11356-013-1659-0.

[44] F. Obiri-Nyarko, S.J. Grajales-Mesa, and G. Malina, *An overview of permeable reactive barriers for in situ sustainable groundwater remediation*, Chemosphere 111 (2014), pp. 243–259. doi:10.1016/j.chemosphere.2014.03.112.

[45] R. Green, T.D. Waite, M.D. Melville, and B.C.T. Macdonald, *Effectiveness of an open limestone channel in treating acid sulfate soil drainage*, Water. Air. Soil Pollut. 191 (2008), pp. 293–304. doi:10.1007/s11270-008-9625-z.

[46] J. Mertens, P. Vervaeke, E. Meers, and F.M.G. Tack, *Seasonal changes of metals in willow (Salix sp.) stands for phytoremediation on dredged sediment*, Environ. Sci. Technol. 40 (2006), pp. 1962–1968. doi:10.1021/es051225i.

[47] C.A. Cravotta, *Size and performance of anoxic limestone drains to neutralize acidic mine drainage*, J. Environ. Qual. 32 (2003), pp. 1277–1289. doi:10.2134/jeq2003.1277.

[48] A. Alcolea, M. Vázquez, A. Caparrós, I. Ibarra, C. García, R. Linares, and R. Rodríguez, *Heavy metal removal of intermittent acid mine drainage with an open limestone channel*, Miner. Eng. 26 (2012), pp. 86–98. doi:10.1016/j.mineng.2011.11.006.

[49] O. Ouakibi, R. Hakkou, and M. Benzaazoua, *Phosphate carbonated wastes used as drains for acidic mine drainage passive treatment*, Procedia Eng. 83 (2014), pp. 407–414. doi:10.1016/j.proeng.2014.09.049.

[50] P.F. Ziemkiewicz, J.G. Skousen, D.L. Brant, P.L. Sterner, and R.J. Lovett, *Acid mine drainage treatment with armored limestone in open limestone channels*, J. Environ. Qual. 26 (1997), pp. 1017–1024. doi:10.2134/jeq1997.00472425002600040013x.

[51] B. Gazea, K. Adam, and A. Kontopoulos, *A review of passive systems for the treatment of acid mine drainage*, Miner. Eng. 9 (1996), pp. 23–42. doi:10.1016/0892-6875(95)00129-8.

[52] E.I. Robbins, C.A. Cravotta, C.E. Savela, and G.L. Nord, *Hydrobiogeochemical interactions in `anoxic' limestone drains for neutralization of acidic mine drainage*, Fuel 78 (1999), pp. 259–270. doi:10.1016/S0016-2361(98)00147-1.

[53] F.M. Kusin, A. Aris, A. Shayeeda, and A. Misbah, *A comparative study of anoxic limestone drain and open limestone channel for acidic raw water treatment*, Int. J. Eng. Technol. 13(6) (2013), pp. 87–92. 133906-8686-IJET-IJENS.

[54] G.R. Watzlaf, K.T. Schroeder, and C.L. Kairies, *Long-term performance of anoxic limestone drains*, Mine Water Environ. 19 (2000), pp. 98–110. doi:10.1007/BF02687258.

[55] C.E. Zipper and J.G. Skousen, *Influent water quality affects performance of passive treatment systems for acid mine drainage*, Mine Water Environ. 29 (2010), pp. 135–143. doi:10.1007/s10230-010-0101-9.

[56] E.R. Goetz and R.G. Riefler, *Performance of steel slag leach beds in acid mine drainage treatment*, Chem. Eng. J. 240 (2014), pp. 579–588. doi:10.1016/j.cej.2013.10.080.

[57] I.Z. Yildirim and M. Prezzi, *Chemical, mineralogical, and morphological properties of steel slag*, Adv. Civ. Eng. (2011), pp. 1–13. doi:10.1155/2011/463638.

[58] D.S. Kumar, M.R.B.S. Subramanya, and S.M.R. Prasad, *Slags aggregates for roads and civil constructions*, National Seminar on New Developments in Alternative Use of Materials, AMCON, Nagpur, India, 2015.

[59] S.D. Cunningham, W.R. Berti, and J.W. Huang, *Phytoremediation of contaminated soils*, Trends Biotechnol. 13 (1995), pp. 393–397. doi:10.1016/S0167-7799(00)88987-8.

[60] H. Deng, Z.H. Ye, and M.H. Wong, *Lead and zinc accumulation and tolerance in populations of six wetland plants*, Environ. Pollut. 141 (2006), pp. 69–80. doi:10.1016/j.envpol.2005.08.015.

[61] A.D. Karathanasis and C.M. Johnson, *Metal removal potential by three aquatic plants in an acid mine drainage wetland*, Mine Water Environ. 22 (2003), pp. 22–30. doi:10.1007/s102300300004.

[62] M. Roy, R. Roychowdhury, P. Mukherjee, A. Roy, B. Nayak, and S. Roy, *Phytoreclamation of abandoned acid mine drainage site after treatment with fly ash*, in *Coal Fly Ash Beneficiation - Treatment of Acid Mine Drainage with Coal Fly Ash*, R. Roychowdhury, ed., IntechOpen, Rijeka, 2018, pp. 111–118. doi:10.5772/intechopen.69527.

[63] C. Garbisu and I. Alkorta, *Phytoextraction: A cost-effective plant-based technology for the removal of metals from the environment*, Bioresour. Technol. 77 (2001), pp. 229–236. doi:10.1016/S0960-8524(00)00108-5.

[64] M. Del Río, R. Font, C. Almela, D. Vélez, R. Montoro, and A. De Haro Bailón, *Heavy metals and arsenic uptake by wild vegetation in the Guadiamar river area after the toxic spill of the Aznalcóllar mine*, J. Biotechnol. 98 (2002), pp. 125–137. doi:10.1016/S0168-1656(02)00091-3.

[65] W. Gwenzi, C.C. Mushaike, N. Chaukura, and T. Bunhu, *Removal of trace metals from acid mine drainage using a sequential combination of coal ash-based adsorbents and phytoremediation by bunchgrass (Vetiver [Vetiveria zizanioides L])*, Mine Water Environ. 36 (2017), pp. 520–531. doi:10.1007/s10230-017-0439-3.

[66] M.M. Lasat, *Phytoextraction of metals from contaminated soil: A review of plant/soil/metal interaction and assessment of pertinent agronomic issues*, J. Hazard. Subst. Res. 2 (1999), pp. 109–120. doi:10.4148/1090-7025.1015.

[67] M.O. Mendez and R.M. Maier, *Phytoremediation of mine tailings in temperate and arid environments*, Rev. Environ. Sci. Biotechnol. 7 (2008), pp. 47–59. doi:10.1007/s11157-007-9125-4.

[68] B. Pivetz, *Phytoremediation of contaminated soil and ground water at hazardous waste sites*, in *groundwater*, Issue, Tech. Rep. EPA/540/S-01/500, United States Environmental Protection Agency, 2001. Available at https://www.epa.gov/sites/production/files/201506/documents/epa_540_s01_500.pdf.

[69] J.S. Weis and P. Weis, *Metal uptake, transport and release by wetland plants: Implications for phytoremediation and restoration*, Environ. Int. 30 (2004), pp. 685–700. doi:10.1016/j.envint.2003.11.002.

[70] G.J. Zagury, C. Neculita, and B. Bussière, *Passive treatment of acid mine drainage in bioreactors: Critical review and research needs*, J. Environ. Qual. 36 (2007), pp. 1–16. doi:10.2134/jeq2006.0066.

[71] O. Gibert, J. de Pablo, J.L. Cortina, and C. Ayora, *Sorption studies of Zn(II) and Cu(II) onto vegetal compost used on reactive mixtures for in situ treatment of acid mine drainage*, Water Res. 39 (2005), pp. 2827–2838. doi:10.1016/j.watres.2005.04.056.

[72] A. Janin and J. Harrington, *Passive treatment of mine drainage waters: The use of biochars and wood products to enhance metal removal efficiency*, Proceedings 2013 Northern Latitudes Mining Reclamation Workshop and 38th Annual Meeting of the Canadian Land Reclamation Association Overcoming Northern Challenge, Whitehorse, Yukon, September 9–12, 2013, pp. 90–99.

[73] T.D. Brock and M.T. Madigan, *Biology of Microorganisms*, 6th ed., Prentice Hall, Englewood Cliffs, New Jersey, 1995.

[74] E.C.M. Kwong, *Abiotic and biotic pyrrhotite dissolution*, MASc Thesis, University of Waterloo, 1995.

[75] B. Lottermoser, *Mine Wates: Characterization, Treatment and Environmental Impacts*, 3rd ed., Springer Science & Business Media, London, 2010.

[76] D. Wagner, *Microbial communities and processes in arctic permafrost environments*, in *Microbiology of Extreme Soils (Soil Biology)*, P. Dion and C. S. Nautiyal, eds., Vol. 13, Springer, Berlin/Heidelberg, 2008, pp. 133–154.

[77] Y. Yang, M. Wan, W. Shi, H. Peng, G. Qiu, J. Zhou, et al., *Bacterial diversity and community structure in acid mine drainage from Dabaoshan Mine, China*, Aquat. Microbiol. Ecol. 47 (2007), pp. 141–151. doi:10.3354/ame047141.

[78] C.S. Kirby and C.A. Cravotta, *Net alkalinity and net acidity 2: Practical considerations*, Appl. Geochem. 20 (2005), pp. 1941–1964. doi:10.1016/j.apgeochem.2005.07.003.

[79] N.A. Kruse, A.L. Mackey, J.R. Bowman, K. Brewster, and R.G. Riefler, *Alkalinity production as an indicator of failure in steel slag leach beds treating acid mine drainage*, Environ. Earth Sci. 67 (2012), pp. 1389–1395. doi:10.1007/s12665-012-1583-5.

[80] S. Santomartino and J.A. Webb, *Estimating the longevity of limestone drains in treating acid mine drainage containing high concentrations of iron*, Appl. Geochem. 22 (2007), pp. 2344–2361. doi:10.1016/j.apgeochem.2007.04.020.

[81] T.R. Lee and R.T. Wilkin, *Iron hydroxy carbonate formation in zerovalent iron permeable reactive barriers: Characterization and evaluation of phase stability*, J. Contam. Hydrol. 116 (2010), pp. 47–57. doi:10.1016/j.jconhyd.2010.05.009.

[82] B.J. Baker and J.F. Banfield, *Microbial communities in acid mine drainage*, FEMS Microbiol. Ecol. 44 (2003), pp. pp. 139–152. doi:10.1016/S0168-6496(03)00028-X.

[83] J. Skousen and P. Ziemkiewicz, *Performance of 116 passive treatment systems for acid mine drainage*, National Meeting of the American Society of Mining and Reclamation, Breckenridge, CO, 2005.

[84] M. Christ, *Operation and maintenance of passive acid mine drainage treatment systems: A framework for watershed groups*, Tech. Rep.Division of Water and Waste Management, Nonpoint Source Program, West Virginia Department of Environmental Protection, Charleston, West Viriginia, 2014.

[85] J. Bolzicco, C. Ayora, T. Rötting, and J. Carrera, *Performance of the Aznalcóllar permeable reactive barrier*, Mine Water Environ., at 8th International Mine Water Conference, Johannesburg, 2003, pp. 287–299.

[86] C. Woulds and B.T. Ngwenya, *Geochemical processes governing the performance of a constructed wetland treating acid mine drainage, Central Scotland*, Appl. Geochem. 19 (2004), pp. 1773–1783. doi:10.1016/j.apgeochem.2004.04.002.

[87] C.D. Barton and A.D. Karathanasis, *Renovation of a failed constructed wetland treating acid mine drainage*, Environ. Geol. 39 (1999), pp. 39–50. doi:10.1007/s002540050435.

CHAPTER 2: COMPARISON OF APTES-FUNCTIONALIZED SILICA FIBER AND CLINOPTILOLITE FOR REMEDIATION OF ACID ROCK DRAINAGE

Submitted to Mine Water and the Environment

Introduction

The generation of acid rock drainage (ARD) from weathering of sulfidic ore and waste rock continues to significantly impact local and regional water resources (Figure 2.1) across the United States and around the globe [1–3]. In particular, abandoned mining sites with degrading infrastructure and uncontrolled entrance of water and oxygen impact water resources in areas that are difficult for reduction or treatment of mine drainage [4]. In an attempt to treat abandoned mine drainage and other sources of poor-quality drainage, passive treatment systems were developed to reduce contaminant concentrations, minimize health risks, and lower treatment costs [4]. Such systems have shown mixed results with treating ARD because of proton (H^+) competition, seasonal flux differences, and variable metal concentrations [5–7], which indicate the need for evaluating additional passive treatment systems and reactive substrates for ARD remediation.

Figure 2.1. Example of acid rock drainage from Stockett, Montana, in the Great Falls Coal Field.

Quality of mine drainage typically is proportional to the acidity of the drainage,[8,9] which is driven by the oxidation of iron-sulfide minerals and subsequent release and mobility of iron [Fe] and other metals [10–14]. Passive treatment of poor-quality mine drainage includes biological, geochemical, and physical processes to improve water quality by reducing acidity and metal concentrations [15]. Inorganic substrates such as calcite, or organic substrates such as organic waste (e.g. mulch), induce metal capture through sorption and(or) changes in acidity and(or) reduction-oxidation potential that induce mineral precipitation [15,16]. Metal capture on inorganic substrates can be viewed as the combination of ligand availability and sorption and(or) precipitation to hydrous oxide surfaces [17–19]. Sorption typically occurs through electrostatic interaction between metals in solution and a negatively charged surface (commonly the oxide of another metal), which can be influenced by surface site availability, sorption of neighboring sites, and cation competition [19].

Metal capture by sorption on silicate substrates, such as zeolites and clays, is common for treatment of waste water [20–22], but silicate options have not typically been used for ARD treatment because of their limited point of zero charge (pH_{pzc}). The presence of competing protons influences the sorption of metals [18,23] through neutralization of the residual negative surface charge (surface protonation) of reactive materials [24]. Artificial and natural silicate substrates such as silica glass and zeolite minerals, tend to have a pH_{pzc} near 3.0 [25,26], which make such substrates applicable to ARD treatment for weak (>4.5) to mildly (>3.0) acidic solutions.

For this study, a manufactured silicate material (fused silica fiber) functionalized with chelator, (3-aminopropyl)triethoxysilane (Si+APTES) and a natural silicate substrate (clinoptilolite [$(Na,K,Ca)_{2–3}Al_3(Al,Si)_2Si_{13}O_{36}\cdot 12H_2O$]) were evaluated at the benchtop scale for potential use in a high-flow ARD passive treatment system. Bare silica fiber was used for comparison as a similar pH_{pzc} without the presence of a chelator. The goal of the study was to determine the potential applicability of these low cost, readily available, and easily prepared substrates for capturing Fe under mildly acidic conditions.

Materials and methods

The selected silica (Si) fiber (Technical Glass Products, Inc., Painesville, Ohio) is a noncrystalline quartz (fused glass) consisting of a wool spun from 5 µm to 15 µm in diameter (Figure 2.2). Specific surface area of the Si fiber (assumed 10 µm diameter) was calculated from a density of 0.016 g/cm, a specific volume of 0.45 cm^3/g, a total length (continuous height (h) (Equation 2.1)) of the fiber in the specific volume equal to 5,787 m/g, which produces a specific surface area (A) of 18 m^2/g (Equation 2.2):

$$h = \frac{V}{\pi r^2} \tag{2.1}$$

$$A = 2\pi rh + 2\pi r^2 \tag{2.2}$$

The Si fiber was factory coated on both sides with a starch binder (4-5% by weight) for ease of handling (Figure 2.2). The weaving of the fiber (wool-like product) provides torsion and bending resistance in a flexible wool that may be manipulated (e.g., rolled, packed) to provide structural resistance to the flow of water.

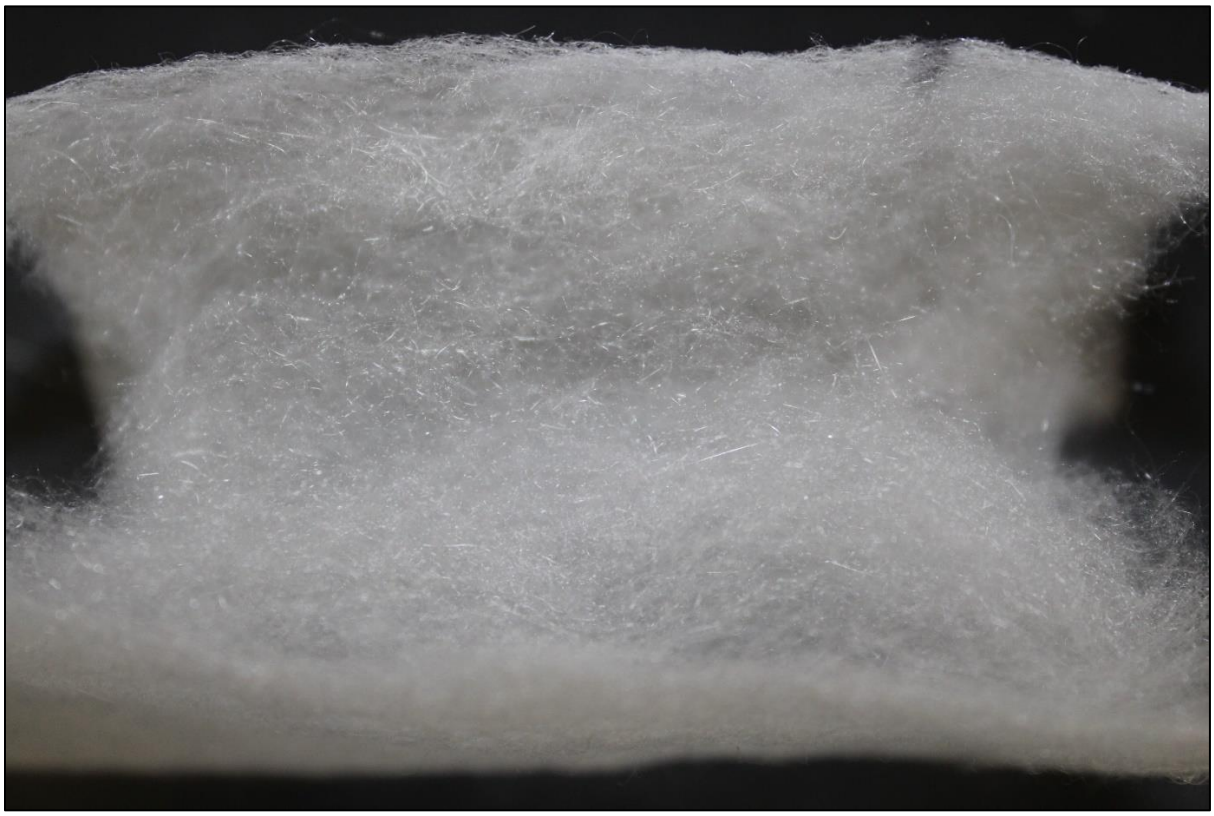

Figure 2.2. Silica fiber spun into a felt; starch coating on top and bottom.

Clinoptilolite (zeolite mineral [hydrated $(Na,K,Ca)_{2\text{-}6}Al_xSi_yO_z$]) are micro-porous aluminosilicate grains derived from volcanic activity but also are synthetically produced [22,27]. Zeolites have the capacity to capture metals through sorption as well as cation exchange and are commonly referred to as "molecular sieves" because of their micropore structure [22,28–31]. For this study, clinoptilolite grains of 2.4 to 4.8 mm in diameter (4 × 8 mesh) were obtained from KMI Zeolite, Inc. in Nevada (Figure 2.3). Specific surface area of the clinoptilolite was determined by the manufacturer to be 40 m^2/g. This type of zeolite typically has a 10- and 8-ring (framework element) micropore structure, which is considered a larger ring (micropore) size in the zeolite mineral family [32]. Prior to experimental use, clinoptilolite grains were triple-rinsed with reverse-osmosis filtered water (ultrapure water) and dried at 80 ºC to remove clinoptilolite dust generated during mining and handling.

Figure 2.3. Clinoptilolite grains, 2.4 to 4.8 mm diameter (4×8 mesh).

Substrate permeability

The permeability of bare Si fiber and the 4 × 8 mesh clinoptilolite were compared through permeability experiments using 5-cm diameter, PVC columns. Permeability experiments were conducted by filling 40-cm (L) columns with either a rolled Si fiber or loosely packed clinoptilolite. Bare Si fiber was tightly rolled and inserted into the column perpendicular to the rolling direction. This configuration allows structural resistance against collapse under the experimental flow

conditions. Si fiber packing densities of 0.073, 0.037, and 0.018 g/cm^3 were tested in this configuration.

Clinoptilolite was poured into the column until grains were freely settled, which produced a packing density of 0.73 g/cm^3. Hydrostatic pressure directed water from a 57 L container, through the 40-cm column and into a collection container (Figure 2.4) where the effluent flow rate was measured. Flow rates were measured after 1 min to allow for full saturation and settling of each substrate. A constant head of 34 L (0.3 m depth) was maintained throughout the experiment with a peristaltic pump that recirculated water from the lower to upper tank. Methylene blue was added as a tracer to the Si fiber permeability experiments for observing possible preferential flow or bypass within the various packing densities.

Figure 2.4. Laboratory setup for permeability column experiments.

Si fiber functionalization

The selected Si fiber represents a synthetic silicate surface that can readily be functionalized with a chelator through a known silanization process where ethoxy groups hydrolyze and form covalent Si-O-Si bonds with the fiber surface [33]. Branched polyethylenimine [$H(NHCH_2CH_2)_nNH_2$] (PEI) and (3-Aminopropyl)triethoxysilane [$C_9H_{23}NO_3Si$] (APTES) were considered for potential use as chelators that could be easily applied to the Si fiber. Preliminary tests indicated greater ease of use (lower viscosity) and superior surface coverage with APTES, which was selected for surface functionalization of the Si fiber for all sorption experiments. The amine functional groups on APTES have proven effective for metal chelation/capture in a variety of solutions [34–36]. APTES was applied to the Si fiber per methods developed by Acres et al. (2012) and Liu et al. (2013) [33,37]. The desired amount of Si fiber was submerged in a 2% APTES (98% EtOH) solution for 20 min while agitated on an orbital shaker. Following submergence and agitation, the Si+APTES was removed and repeatedly rinsed with 100% EtOH and ultrapure water. Rinsed Si+APTES were dried in an oven at 80 ºC for 15 hours. Si surfaces were not treated with an oxidizer, such as piranha solution (mixture of H_2SO_4 and H_2O_2), prior to functionalization [37,38] because such a step would have removed the starch coating that is crucial to its structural integrity for ease of handling and packing.

Preparation of acidic Fe^{2+} stock solutions

Acidic Fe^{2+} solutions were prepared for sorption experiments at Fe concentrations of 25 to 1,000 mg/L by dissolving an appropriate mass of ferrous-sulfate heptahydrate [$FeSO_4 \cdot 7H_2O$] in ultrapure water. Sulfuric acid [H_2SO_4] was added to solutions until an initial pH of 3.0 was obtained and stable while solutions were mixed on an orbital shaker at 100 rpm for 30 minutes.

Batch sorption experiments

Batch sorption experiments were conducted on equivalent surface areas (216 m^2) of each substrate by inserting 12 g of Si, 12 g of Si+APTES, and 5.4 g of clinoptilolite within polyester mesh bags (three replicates) and suspending them in acidic Fe^{2+} solutions [25, 50, 75, 100 mg/L] at 25 ºC. Solutions were continuously agitated on an orbital shaker at 100 rpm, and a pH of 3.00 ± 0.10 was maintained throughout each experiment by introduction of H_2SO_4 (monitored by pH probe). The substrates were suspended in the acidic Fe^{2+} solutions in 1-L beakers and agitated on a shaker table for 4 to 6 hr until sorption equilibrium occurred (stabilization of solution Fe concentration). Fe concentrations were measured with a Hach 3900 spectrophotometer and FerroVer reagent. Quality control and accuracy checks were performed over the course of the experiments with instrument

blanks, replicate samples, and calibration standards. No false positive results were indicated, and replicate results were within acceptable range (±10%) for Fe concentration. Specific sorption values (q; mg/g) were calculated for batch and column sorption experiments:

$$q = \frac{C_i - C_f}{M} \quad (2.3)$$

where C_i and C_f are initial and final concentrations of Fe (mg/L), respectively, and M is substrate mass (mg/L).

Adsorption isotherms

Specific sorption values for each substrate were compared to Langmuir and Freundlich isotherm models to evaluate possible sorption characteristics. The Langmuir isotherm model assumes a homogeneous surface with a finite number of monolayer sorption sites [39]:

$$q_e = q_{max}\frac{K_L C_e}{1 + K_L C_e} \quad (2.4)$$

where q_e is amount adsorbed (mg/g) at an equilibrium concentration C_e (mg/L), q_{max} is maximum monolayer adsorption (mg/g), and K_L is the Langmuir constant related to free energy of adsorption [28].

The Freundlich isotherm model assumes a heterogeneous surface where adsorption can occur in multiple layers [28,40,41].

$$q_e = K_f C_e^{1/n} \quad (2.5)$$

where K_f is the Freundlich constant related to maximum adsorption capacity (mg/g) and n is a constant related to adsorption intensity [28,42].

Small-scale column experiments

Small-scale column experiments were conducted by inserting 15 g of Si+APTES or 150 g of clinoptilolite (packing densities of 0.073 and 0.73 g/cm^3, respectively) within a PVC column of 5-cm diameter × 10-cm length (Figure 2.5). Si+APTES was tightly rolled into a cylinder form prior to insertion into the column to provide sufficient structural integrity during wetting, and maximizing surface area availability. A peristaltic pump directed acidic Fe^{2+} solution (1,000 mg/L) to the bottom of the flow column, through the permeable substrates, out the top of the column, and into a waste container at a rate of 25 mL/min and 12 mL/min for Si+APTES and clinoptilolite, respectively (slowest possible rate given resistance to flow). Effluent solution was collected at 0, 7.5, 15, 30, 60,

90, 120, 150, 180, 240, 300, and 360 minutes. Fe concentration was measured with a Hach DR3900 spectrophotometer until sorption site exhaustion of each substrate (effluent Fe concentration equal to influent concentration). Three replicate experiments were conducted in sequential order for each substrate. Following each experiment, the experimental apparatus was cleaned in a 15% HNO_3 bath and rinsed with ultrapure water.

Figure 2.5. Example of small-scale column experiment.

In both small- and large-scale column experiments the concentration of removed Fe was found by subtracting effluent Fe concentration from influent Fe concentration. The area under the breakthrough curve attained by integrating the removed concentration (C_{rem}; mg/L) versus time (min) plot can be used to find the total Fe removed (R_{total}; mg) in the column for a given pumping rate (Q) (Equation 2.6) [43].

$$R_{total} = \frac{Q}{1000} \int_{t=0}^{t=t_{total}} C_{rem}\, dt \tag{2.6}$$

Large-scale column experiments

Large-scale column experiments were conducted by inserting 600 g of clinoptilolite (0.73 g/cm^3 packing density) within a PVC column of 5-cm diameter × 40-cm length (Figure 2.6). A peristaltic pump directed acidic Fe^{2+} solution (1,000 mg/L) to the bottom of the flow column, through the permeable substrates, out the top of the column, and into a waste container at a rate of 12 mL/min. Effluent solution was collected at 0, 0.5, 0.75, 1, 1.5, 2, 4, 6, 8, 14, 20, 26, 32, 38, 44, 50, 56, 62, 68, 74, 80, 86, 92, 98, and 104 hr. Total Fe concentration was measured with a Hach DR3900 spectrophotometer until surface site exhaustion (influent concentration = effluent concentration). Large-scale column experiments were conducted sequentially in triplicate.

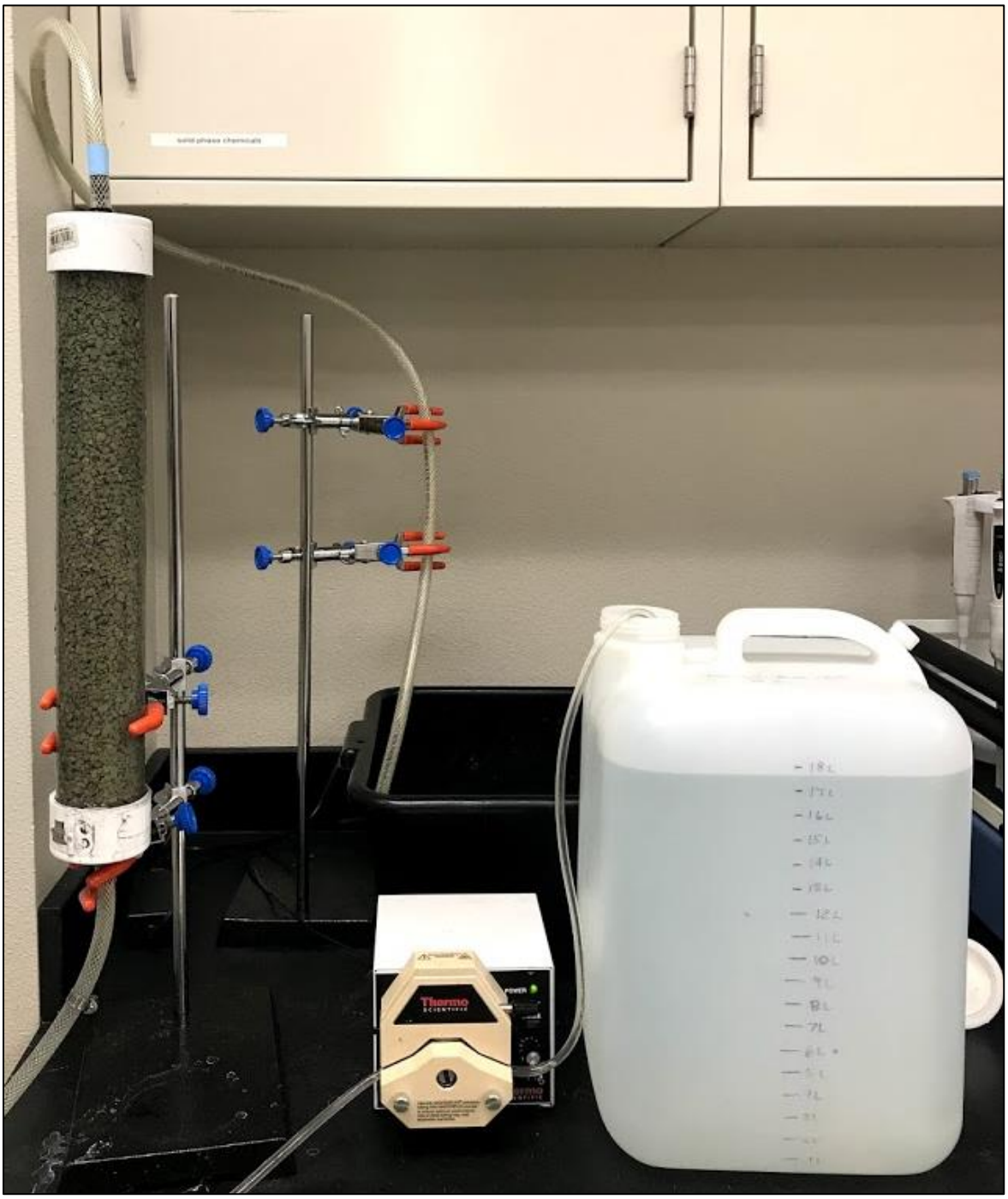

Figure 2.6. Example of large-scale column experiment.

Clinoptilolite surface analysis

Pre- and post-experiment clinoptilolite surface morphology and Fe distribution were analyzed using a scanning electron microscope (Zeiss SUPRA 35 SEM) equipped with energy dispersive x-ray

spectroscopy (Noran System Six EDS) at the University of Idaho Electron Microscopy Center. Samples were carbon-coated prior to analysis. Clinoptilolite surfaces were imaged for an evaluation of potential changes in surface morphology pre- and post-experiment and distribution of captured Fe across the grain surface.

Results and discussion

Permeability comparison

Permeability results indicate that clinoptilolite at a 4 × 8 mesh grain size has a greater permeability that Si fiber at all packing densities tested. Measured flow rates through Si fiber at packing densities of 0.073, 0.037, and 0.018 g/cm^3 were 0.06, 0.08, and 0.14 L/s, respectively. Results indicate that flow rate increased at lower packing densities; however, methylene blue dye tracers revealed that preferential flow was occurring within the column at packing densities of 0.037 and 0.018 g/cm^3. Si fiber at a packing density of 0.073 g/cm^3 resulted in a supportable and permeable packing arrangement that did not induce flow bypass. In all cases, Si fiber retained water in void space, restricting permeability.

Clinoptilolite grains were slightly compacted after saturation, but permeability remained at 0.20 L/s for the duration of the experiment. This flow rate is nearly three times the flow rate allowed by Si fiber at 0.073 g/cm^3. From the permeability results, packing densities of 0.073 g/cm^3 for Si fiber and Si+APTES, and 0.73 g/cm^3 for clinoptilolite were selected for use in batch sorption calculations and column experiments.

Batch sorption comparison and adsorption isotherms

Specific sorption of Fe^{2+} by bare Si fiber was minimal for all Fe concentrations; therefore, further experimentation with bare Si fiber was abandoned. Sorption of Fe on Si+APTES and clinoptilolite increased as Fe concentration increased (Figure 2.7). Specific sorption of Fe^{2+} at all concentrations was greater for Si+APTES compared to clinoptilolite (Figure 2.7). Specific sorption values are not indicative of how the substrates would perform in a passive treatment system because a greater mass (and surface area) of clinoptilolite could be packed into a similar volume and retain permeability compared to Si+APTES. For this reason, specific sorption values were multiplied by packing densities of 0.073 and 0.73 g/cm^3 for Si+APTES and clinoptilolite, respectively (Figure 2.8). Results indicate that a greater amount of Fe^{2+} was sorbed per volume (mg/cm^3) for clinoptilolite compared to Si+APTES (Figure 2.8).

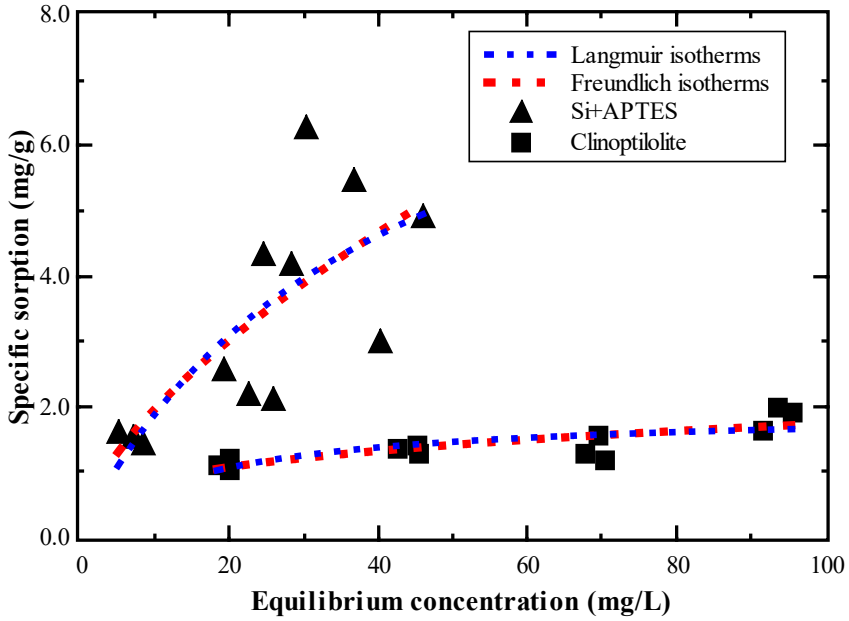

Figure 2.7. Equivalent surface area adsorption equilibria of Fe^{2+} on Si+APTES and clinoptilolite at pH of 3.0 and Fe concentrations of 25, 50, 75, 100 mg/L with associated Langmuir and Freundlich isotherm curves.

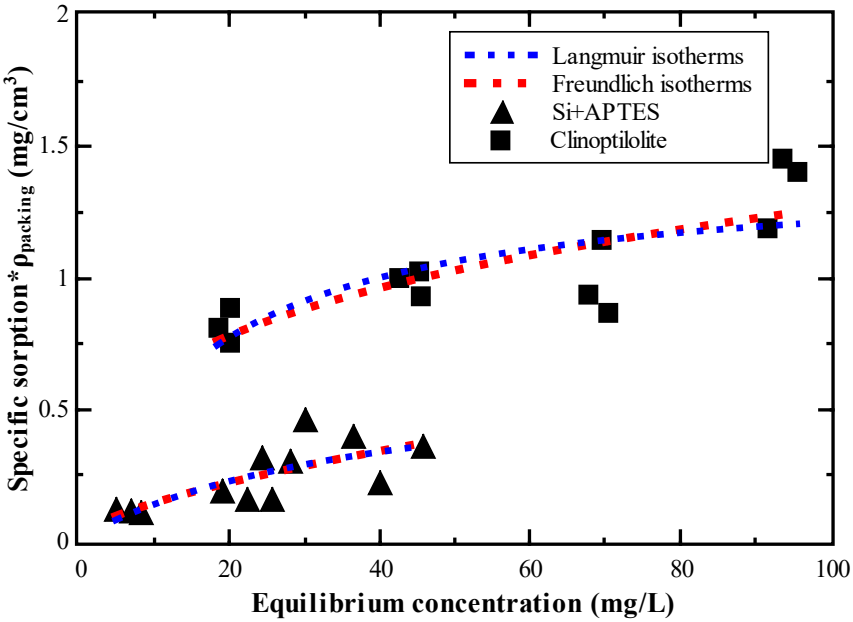

Figure 2.8. Packing density normalized adsorption equilibria of Fe^{2+} on Si+APTES and clinoptilolite at pH of 3.0 and Fe concentrations of 25, 50, 75, 100 mg/L with associated Langmuir and Freundlich isotherm curves.

Neither the Langmuir or Freundlich isotherms were representative of the specific sorption results for Si+APTES and clinoptilolite. R^2 values calculated for the Langmuir isotherm were 0.545 and 0.544 for Si+APTES and clinoptilolite, respectively (Table 2.1). The chelating functional group of Si+APTES and the microporous structure of clinoptilolite create heterogeneous surfaces, and sorption likely is not occurring in a monolayer as predicted by the Langmuir model. R^2 values calculated for the Freundlich isotherm were 0.541 and 0.632 for Si+APTES and clinoptilolite, respectively (Table 1). The Freundlich model does not represent metal capture by Si+APTES because Fe removal is occurring by sorption and chelation rather than just adsorption. The Freundlich model is a better fit for clinoptilolite because the model assumes a heterogeneous surface where multilayer sorption can occur, which is an applicable assumption for the variable topography of a clinoptilolite surface. Overall, neither model is appropriate to fully describe metal removal by Si+APTES or clinoptilolite surfaces, which also may be a result of Fe precipitation processes in addition to sorption. All post-experiment Si+APTES and clinoptilolite surfaces indicated a color change (Figure 2.9) suggestive of Fe-(oxyhydr)oxide precipitation as a result of capture and interaction with the substrate surfaces.

Table 2.1. Parameter estimates for Langmuir and Freundlich isotherm models for experimental results of Fe^{2+} adsorption on Si+APTES and clinoptilolite at a solution pH of 3.0.

Model type	**Si+APTES**	**Clinoptilolite**
Langmuir isotherm		
K_l[a] (L/mg)	0.024 ± 0.028	0.061 ± 0.027
q_{max}[b] (mg/g)	9.225 ± 6.164	1.936 ± 0.214
R^2[c]	0.545	0.544
Freundlich isotherm		
K_f[d] (mg/g)	0.436 ± 0.356	0.436 ± 0.135
n[e]	1.564 ± 0.590	3.337 ± 0.849
R^2	0.541	0.632

[a]K_L= Langmuir constant related to free energy of adsorption. [b]q_{max} = maximum monolayer adsorption. [c]R^2 = coefficient of determination. [d]K_f = Freundlich constant related to maximum adsorption. [e]n = constant related to sorption intensity.

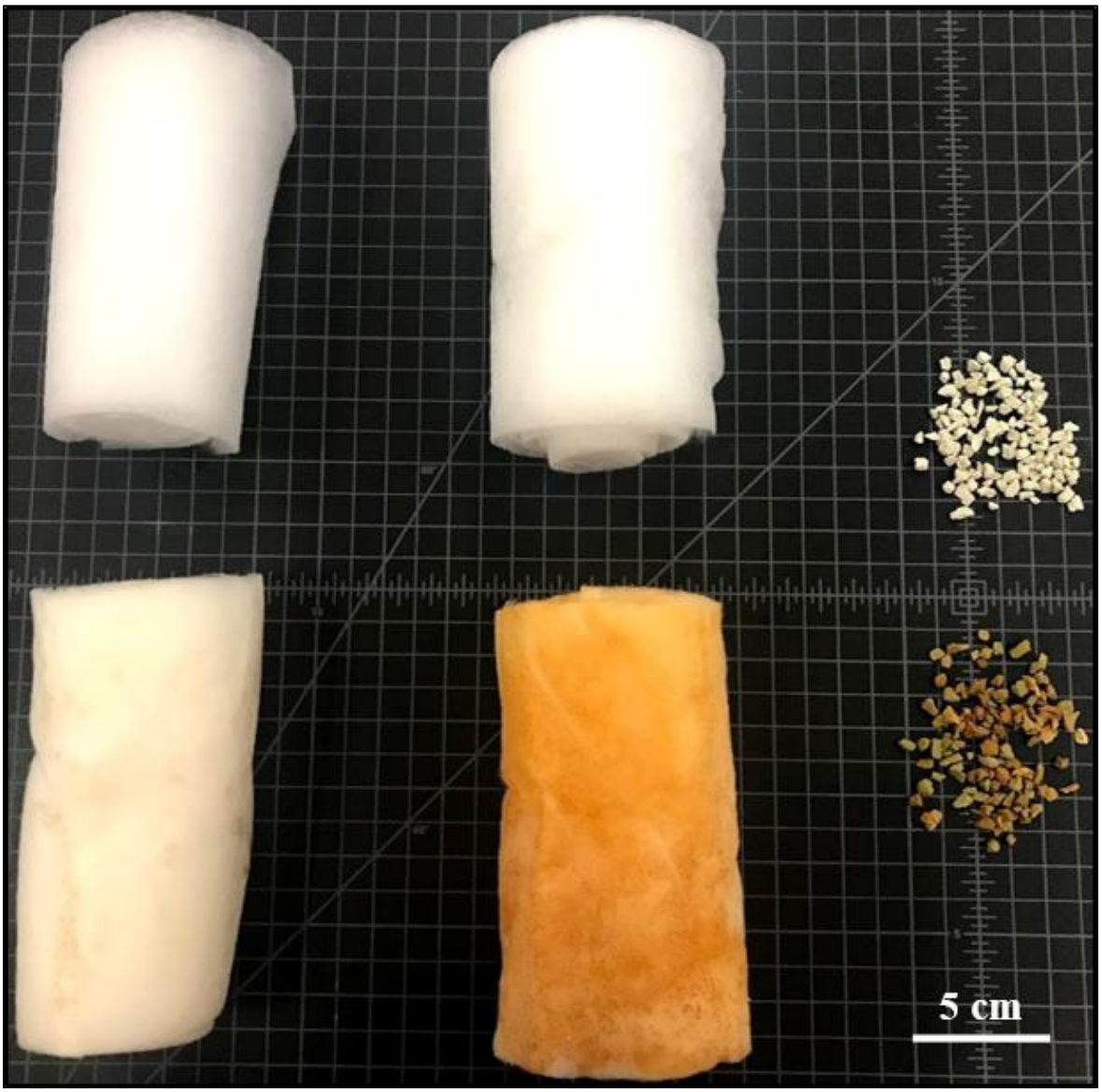

Figure 2.9. (Left to right) 12 g of Si, 12 g of Si+APTES, and 5.4 g of clinoptilolite before (top row) and after (bottom row) batch sorption experiments. Orange color is due to sorbed/precipitated iron-(oxyhydr)oxides.

Column experiments

Results from small-scale column experiments with 150 g of clinoptilolite (6,000 m^2 surface area), 15 g of Si + APTES (270 m^2 surface area), and 1,000 mg/L Fe solutions indicate greater Fe removal by clinoptilolite, with sorption site exhaustion occurring at approximately 60 minutes for Si+APTES and 360 minutes for clinoptilolite (Figure 2.10). Values for total Fe removal (R_{total}) were normalized by substrate mass and surface area, indicating equivalent Fe removal per g (R_M; mg/g) for

both substrates, and a greater Fe removal per m^2 of surface area (R_{SA}) for Si+APTES (Table 2.2). For both substrates, Fe-(oxyhydr)oxide precipitation occurred because of unidentified acid-neutralizing processes, resulting in rapid increases in effluent pH from 3.0 to 6.3 for Si+APTES and 3.0 to 5.9 for clinoptilolite (Figure 2.11). As small-scale column experiments continued, effluent pH gradually decreased to 3.0 for Si+APTES and 3.4 for clinoptilolite after 360 minutes (Figure 2.11).

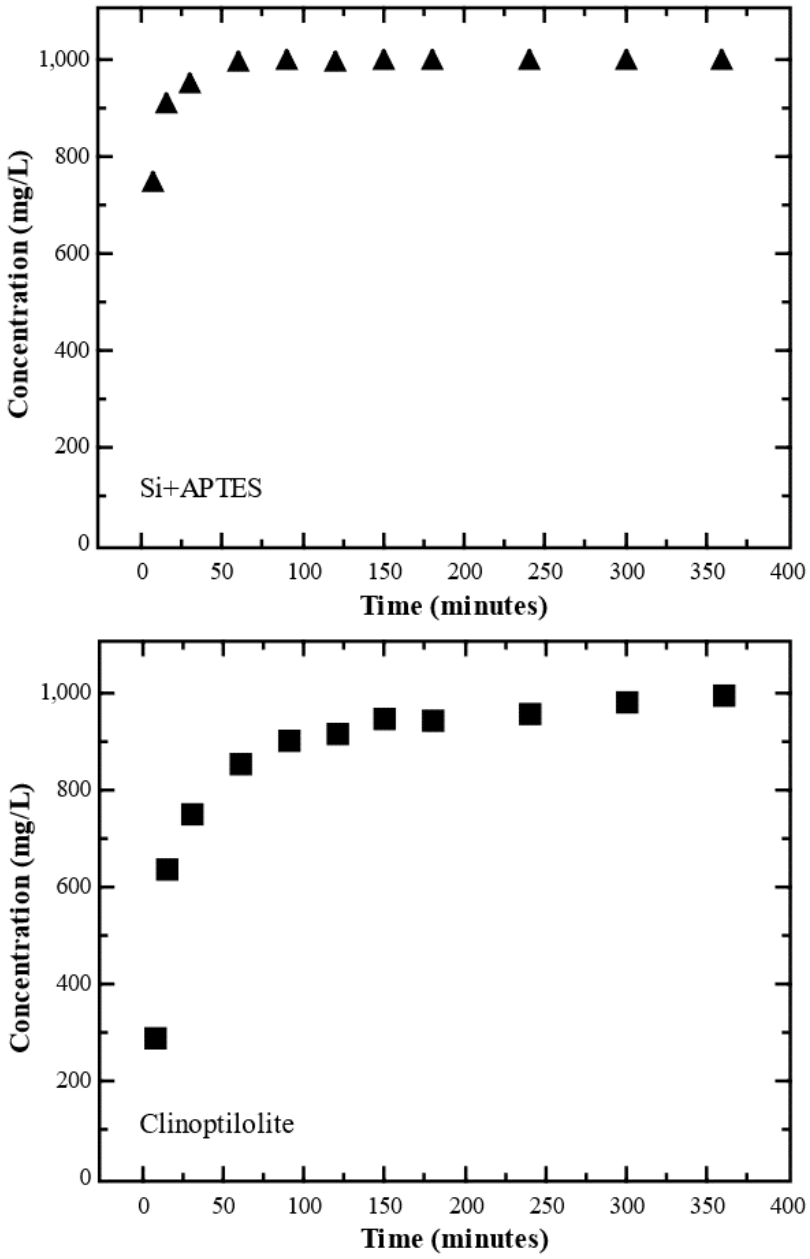

Figure 2.10. Sorption of Fe^{2+} to Si+APTES (left) and clinoptilolite (right) in small-scale column experiments.

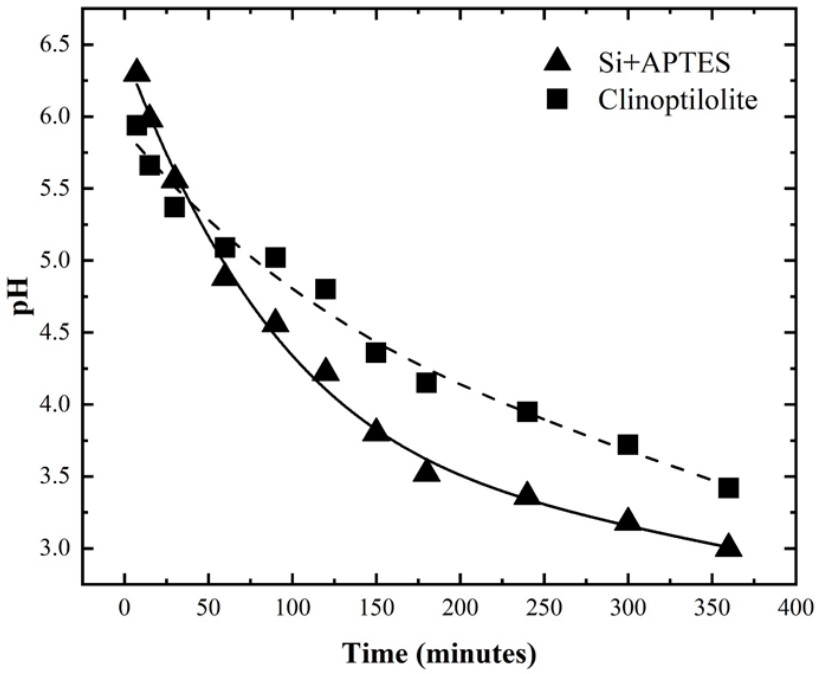

Figure 2.11. pH change over the course of small-scale column experiments. Initial pH of solution was 3.0 ± 0.1.

Given greater permeability and greater normalized Fe removal for clinoptilolite, large-scale column experiments were used to evaluate potential changes in Fe removal with an increase in flowpath length through the same loosely packed, clinoptilolite grain structure. Results indicate that quadrupling the amount of clinoptilolite from small to large column experiments increased time to exhaustion by a factor of 17 (Figure 2.12). Normalized R_{total} values indicate that the longer flowpath length of the large-scale column experiments increased Fe removal by nearly 50 mg/g and 1.5 mg/m^2 (Table 2.2). Initial column effluent increased in pH from 3.0 to 7.0, resulting in Fe-(oxyhydr)oxide precipitation, followed by a gradual decrease of pH to 3.7 by the end of the experiments (Figure 2.12).

Table 2.2. Results from large- and small-scale column experiments.

Substrate	Mass (g)	SA[a] (m^2)	R_{total}[b] (mg)	R_M[c] (mg/g)	R_{SA}[d] (mg/m^2)
Small-scale column					
Si+APTES	15	270	137	9.1	0.5
Clinoptilolite	150	6,000	1,364	9.1	0.2
Large-scale column					
Clinoptilolite	600	24,000	40,302	67.2	1.7

[a]SA = square meters of surface area. [b]R_{total} = total milligrams of iron removed. [c]R_M = milligrams of iron removed per g of substrate. [d]R_{SA} = milligrams of iron removed per square meter of substrate surface area.

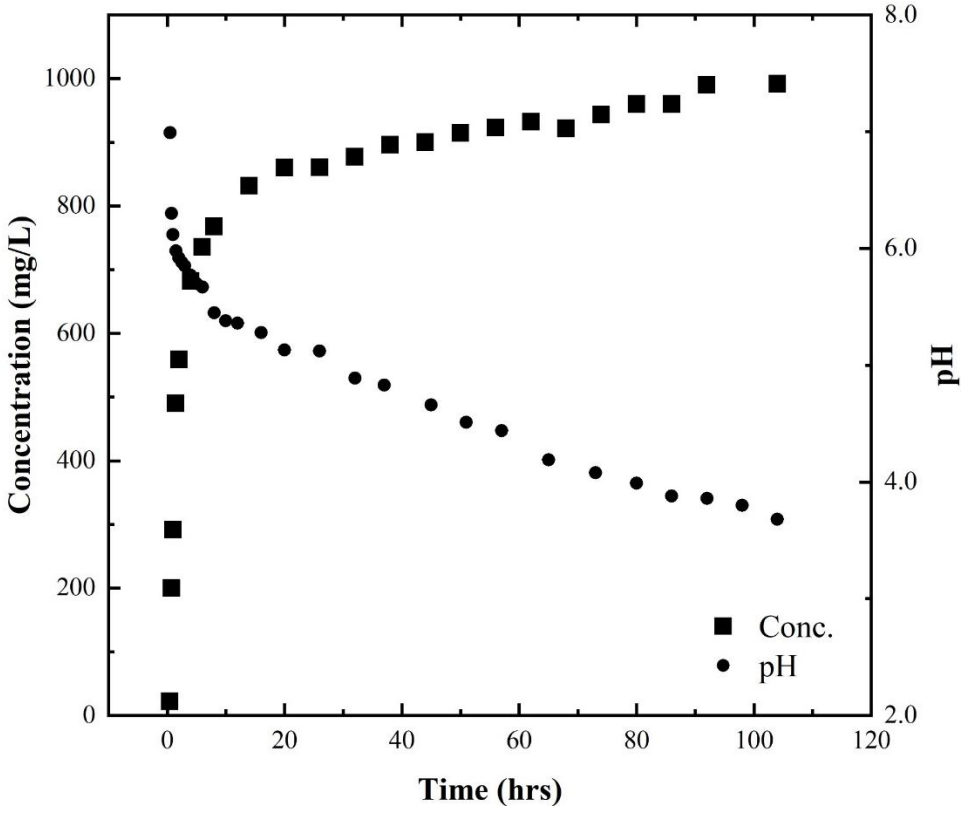

Figure 2.12. Change in Fe^{2+} concentration and pH during large-scale column experiments. Initial pH of solution was 3.0 ± 0.1.

Column experimental trend comparison

In both small- and large-scale column experiments, Fe removal was initially high and decreased exponentially, followed by a linear trend in surface passivation with continual Fe removal (Figures 2.10 and 2.12). The large removal of Fe from solution during the initial period of the small- and large-scale column experiments likely is a result of the corresponding change in pH, which decreased Fe solubility and resulted in precipitation of Fe-(oxyhydr)oxides [44]. Subsequently, these Fe-(oxyhydr)oxides potentially provided additional surfaces for Fe sorption to occur [45]. The ensuing period of a gradual increase in Fe concentration in solution and decrease in pH likely is reflective of the decrease in sorption sites as the surface and pores become saturated with sorbed and precipitated Fe (Figures 2.10 and 2.12) [46]. Fe removal did not scale according to an increase in mass or surface area between small- and large-scale column experiments (Table 2.2). Fe removal by clinoptilolite increased substantially on a normalized comparison from small- to large-scale column experiments as a result of longer flowpaths and greater interaction with clinoptilolite (Table 2.2).

SEM analysis

The irregular surface topography and its microporous structures result in large surface areas available for sorption of ions [22]. A post-experiment evaluation of Fe distribution on the surface of clinoptilolite indicates a diffuse capture of Fe across the clinoptilolite surface (Figure 2.13). There were concentrated areas of Fe capture but no obvious patterns of Fe distribution across the grain surface that indicate greater capture on any topographic area or large accumulations suggestive of primary areas of mineral precipitation and growth. The entire clinoptilolite surface of the grains appear to have been available for metal removal through sorption and precipitation.

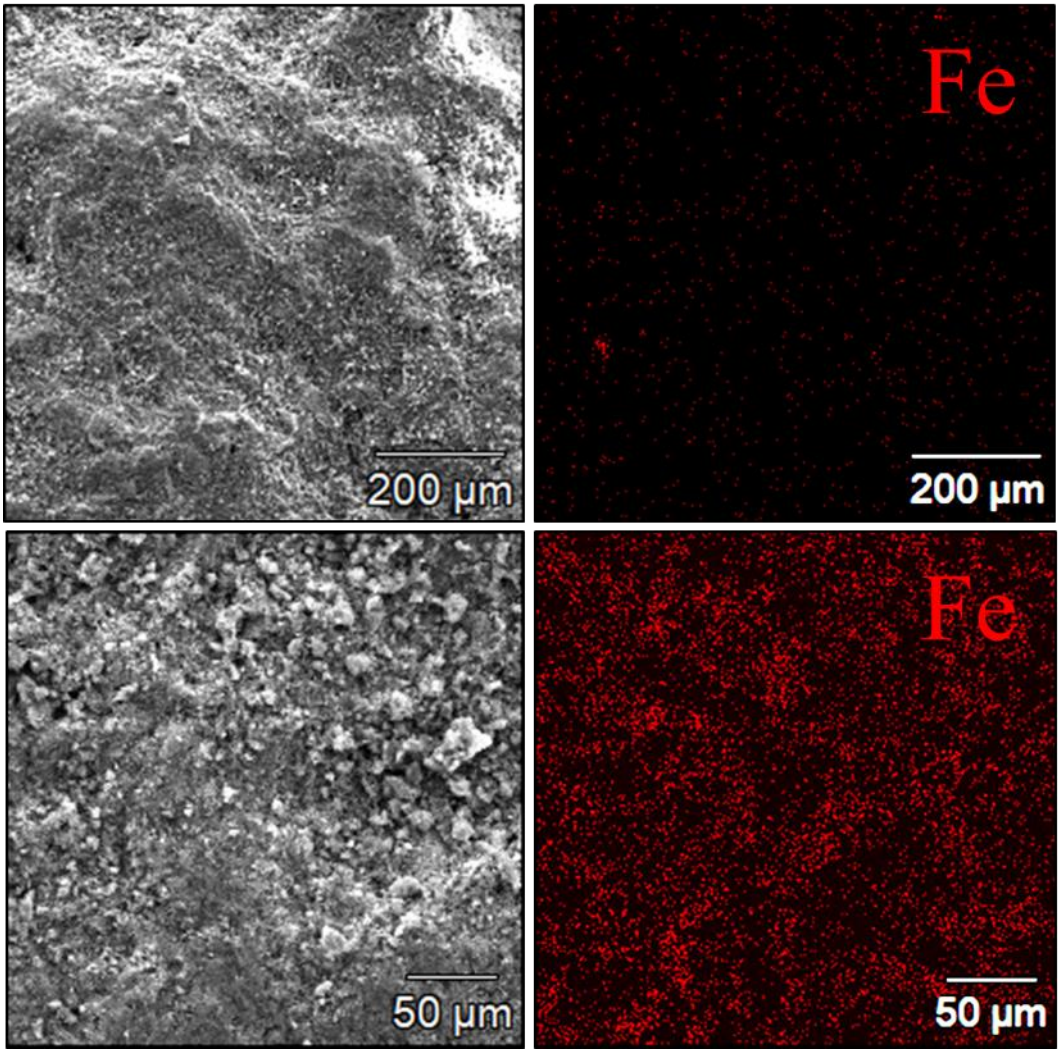

Figure 2.13. (Top row) SEM image of pre-experiment clinoptilolite surface at 137× magnification with corresponding EDS spectral map of Fe. (Bottom row) SEM image of post-experiment clinoptilolite surface at 380× magnification with corresponding EDS spectral map of Fe. Kα peak was used for element identification.

Substrate selection

Si+APTES demonstrated high specific sorption of Fe in batch sorption experiments and has potential use in low-flow ARD passive treatment systems. The balance of greater packing stability and permeability, large surface area, microporous structure, and ion-exchange properties of clinoptilolite make these natural zeolite grains a better reactive substrate for passive treatment of acidic drainage in high- or low-flow conditions. Furthermore, surface preparation is minimal for clinoptilolite and as a readily available substrate, it can easily be incorporated into construction of passive treatment systems.

References

[1] A. Akcil and S. Koldas, *Acid Mine Drainage (AMD): causes, treatment and case studies*, J. Clean. Prod. 14 (2006), pp. 1139–1145. doi:10.1016/j.jclepro.2004.09.006.

[2] S.G. Benner, D.W. Blowes, W.D. Gould, Herbert R.B. and C.J. Ptacek, *Geochemistry of a permeable reactive barrier for metals and acid mine drainage*, Environ. Sci. Technol. 33 (1999), pp. 2793–2799. doi:10.1021/es981040u.

[3] D.K. Nordstrom, *Acid rock drainage and climate change*, J. Geochem. Explor. 100 (2009), pp. 97–104. doi:10.1016/j.gexplo.2008.08.002.

[4] D.B. Johnson and K.B. Hallberg, *Acid mine drainage remediation options: A review*, Sci. Total Environ. 338 (2005), pp. 3–14. doi:10.1016/j.gexplo.2008.08.002.

[5] C. Costello, *Acid mine drainage: Innovative treatment technologies*, US EPA Office of Solid Waste and Emergency Response Technology Innovation Office, Washington, DC, 2003.

[6] A.E. Fryar and F.W. Schwartz, *Hydraulic-conductivity reduction, reaction-front propagation, and preferential flow within a model reactive barrier*, J. Contam. Hydrol. 32 (1998), pp. 333–351. doi:10.1016/S0169-7722(98)00057-6.

[7] W. Sandlin, J. Langman and J. Moberly, *A review of acid rock drainage, seasonal flux of discharge and metal concentrations, and passive treatment system limitations*, Int. J. Min. Reclam. Environ. (2020), pp. 1–14. doi:10.1080/17480930.2020.1728035.

[8] K.K. Kefeni, T.A.M. Msagati and B.B. Mamba, *Acid mine drainage: Prevention, treatment options, and resource recovery: A review*, J. Clean. Prod. 151 (2017), pp. 475–493. doi:10.1016/j.jclepro.2017.03.082.

[9] D.K. Nordstrom and C.N. Alpers, *Negative pH, efflorescent mineralogy, and consequences for environmental restoration at the Iron Mountain Superfund site, California*, Proc. Natl. Acad. Sci. 96 (1999), pp. 3455–3462. doi:10.1073/pnas.96.7.3455.

[10] J.M. Bigham and D.K. Nordstrom, *Iron and aluminum hydroxysulfates from acid sulfate waters*, Rev. Mineral. Geochem. 40 (2000), pp. 351–403. doi:10.2138/rmg.2000.40.7.

[11] B. Dold, *Acid rock drainage prediction: A critical review*, J. Geochem. Explor. 172 (2017), pp. 120–132. doi:10.1016/j.gexplo.2016.09.014.

[12] N.O. Egiebor and B. Oni, *Acid rock drainage formation and treatment: a review*, Asia-Pac. J. Chem. Eng. 2 (2007), pp. 47–62. doi:10.1002/apj.57.

[13] D.K. Nordstrom, *Mine Waters: Acidic to Circumneutral*, Elements 7 (2011), pp. 393–398. doi:10.2113/gselements.7.6.393.

[14] D.K. Nordstrom, D.W. Blowes and C.J. Ptacek, *Hydrogeochemistry and microbiology of mine drainage: An update*, Appl. Geochem. 57 (2015), pp. 3–16. doi:10.1016/j.apgeochem.2015.02.008.

[15] J. Skousen, C.E. Zipper, A. Rose, P.F. Ziemkiewicz, R. Nairn, L.M. McDonald et al., *Review of passive systems for acid mine drainage treatment*, Mine Water Environ. 36 (2017), pp. 133–153. doi:10.1007/s10230-016-0417-1.

[16] O. Gibert, J. de Pablo, J. Luis Cortina and C. Ayora, *Chemical characterisation of natural organic substrates for biological mitigation of acid mine drainage*, Water Res. 38 (2004), pp. 4186–4196. doi:10.1016/j.watres.2004.06.023.

[17] J.A. Davis and J.O. Leckie, *Surface ionization and complexation at the oxide/water interface II. Surface properties of amorphous iron oxyhydroxide and adsorption of metal ions*, J. Colloid Interface Sci. 67 (1978), pp. 90–107. doi:10.1016/0021-9797(78)90217-5.

[18] D.A. Dzombak and F.M.M. Morel, *Surface complexation modeling: Hydrous ferric oxide*, John Wiley & Sons, Inc., 1990.

[19] W. Stumm and J.J. Morgan, *Aquatic chemistry: Chemical equilibria and rates in natural waters*, 3rd ed.John Wiley & Sons, Inc., 1996.

[20] H. Faghihian, M. Ghannadi Marageh and H. Kazemian, *The use of clinoptilolite and its sodium form for removal of radioactive cesium, and strontium from nuclear wastewater and* Pb^{2+}, Ni^{2+}, Cd^{2+}, Ba^{2+} *from municipal wastewater*, Appl. Radiat. Isot. 50 (1999), pp. 655–660. doi:10.1016/S0969-8043(98)00134-1.

[21] Ö. Yavuz, Y. Altunkaynak and F. Güzel, *Removal of copper, nickel, cobalt and manganese from aqueous solution by kaolinite*, Water Res. 37 (2003), pp. 948–952. doi:10.1016/S0043-1354(02)00409-8.

[22] I. Pandová, A. Panda, J. Valíček, M. Harničárová, M. Kušnerová and Z. Palková, *Use of sorption of copper cations by clinoptilolite for wastewater treatment*, Int. J. Environ. Res. Public. Health 15 (2018), pp. 1364. doi:10.3390/ijerph15071364.

[23] I. Heidmann, I. Christl and R. Kretzschmar, *Sorption of Cu and Pb to kaolinite-fulvic acid colloids: Assessment of sorbent interactions*, Geochim. Cosmochim. Acta 69 (2005), pp. 1675–1686. doi:10.1016/j.gca.2004.10.002.

[24] J. Nelson, C. Joe-Wong and K. Maher, *Cr(VI) reduction by Fe(II) sorbed to silica surfaces*, Chemosphere 234 (2019), pp. 98–107. doi:10.1016/j.chemosphere.2019.06.039.

[25] G.M. Gainer, *Boron adsorption on hematite and clinoptilolite*, Tech. Rep. LA SUB-93-64, Los Alamos, 1993.

[26] A. Cotton, *Dissolution kinetics of clinoptilolite and heulandite in alkaline conditions*, Biosci. Horiz. 1 (2008), pp. 38–43. doi: 10.1093/biohorizons/hzn003.

[27] A.E. Burakov, E.V. Galunin, I.V. Burakova, A.E. Kucherova, S. Agarwal, A.G. Tkachev et al., *Adsorption of heavy metals on conventional and nanostructured materials for wastewater treatment purposes: A review*, Ecotoxicol. Environ. Saf. 148 (2018), pp. 702–712.

[28] M. Holub, M. Balintova, P. Pavlikova and L. Palascakova, *Study of sorption properties of zeolite in acidic conditions in dependence on particle size*, Ital. Assoc. Chem. Eng. 32 (2013), pp. 559–564.

[29] T. Motsi, N.A. Rowson and M.J.H. Simmons, *Adsorption of heavy metals from acid mine drainage by natural zeolite*, Int. J. Miner. Process. 92 (2009), pp. 42–48. doi:10.1016/j.minpro.2009.02.005.

[30] M.A. Stylianou, M.P. Hadjiconstantinou, V.J. Inglezakis, K.G. Moustakas and M.D. Loizidou, *Use of natural clinoptilolite for the removal of lead, copper and zinc in fixed bed column*, J. Hazard. Mater. 143 (2007), pp. 575–581.

[31] S. Wang and Y. Peng, *Natural zeolites as effective adsorbents in water and wastewater treatment*, Chem. Eng. J. 156 (2010), pp. 11–24.

[32] C. Baerlocher, L.B. McCusker and D.H. Olson, *Atlas of Zeolite Framework Types*, 6th rev. ed, Elsevier, Amsterdam, 2007.

[33] Y. Liu, Y. Li, X.-M. Li and T. He, *Kinetics of (3-Aminopropyl)triethoxylsilane (APTES) Silanization of Superparamagnetic Iron Oxide Nanoparticles*, Langmuir 29 (2013), pp. 15275–15282. doi:10.1021/la403269u.

[34] K.N. Barquist, *Synthesis and environmental adsorption applications of functionalized zeolites and iron oxide/zeolite composites*, PhD thesis, University of Iowa, 2009.

[35] D.L. Ramasamy, S. Khan, E. Repo and M. Sillanpää, *Synthesis of mesoporous and microporous amine and non-amine functionalized silica gels for the application of rare earth elements (REE) recovery from the waste water-understanding the role of pH, temperature, calcination and mechanism in Light REE and Heavy REE separation*, Chem. Eng. J. 322 (2017), pp. 56–65. doi:10.1016/j.cej.2017.03.152.

[36] D.L. Ramasamy, V. Puhakka, S. Iftekhar, A. Wojtuś, E. Repo, S. Ben Hammouda et al., *N- and O- ligand doped mesoporous silica-chitosan hybrid beads for the efficient, sustainable and selective recovery of rare earth elements (REE) from acid mine drainage (AMD): Understanding the significance of physical modification and conditioning of the polymer*, J. Hazard. Mater. 348 (2018), pp. 84–91. doi:10.1016/j.jhazmat.2018.01.030.

[37] R.G. Acres, A.V. Ellis, J. Alvino, C.E. Lenahan, D.A. Khodakov, G.F. Metha et al., *Molecular structure of 3-aminopropyltriethoxysilane layers formed on silanol-terminated silicon surfaces*, J. Phys. Chem. C 116 (2012), pp. 6289–6297. doi:10.1021/jp212056s.

[38] M. Zhu, M.Z. Lerum and W. Chen, *How to prepare reproducible, homogeneous, and hydrolytically stable aminosilane-derived layers on silica*, Langmuir 28 (2012), pp. 416–423. doi:10.1021/la203638g.

[39] I. Langmuir, *The adsorption of gases on plane surfaces of glass, mica and platinum*, J. Am. Chem. Soc. 40 (1918), pp. 1361–1403. doi:10.1021/ja02242a004.

[40] G. Limousin, J.-P. Gaudet, L. Charlet, S. Szenknect, V. Barthès and M. Krimissa, *Sorption isotherms: A review on physical bases, modeling and measurement*, Appl. Geochem. 22 (2007), pp. 249–275. doi:10.1016/j.apgeochem.2006.09.010.

[41] E. Erdem, N. Karapinar and R. Donat, *The removal of heavy metal cations by natural zeolites*, J. Colloid Interface Sci. 280 (2004), pp. 309–314. doi:10.1016/j.jcis.2004.08.028.

[42] C. Fan and Y. Zhang, *Adsorption isotherms, kinetics and thermodynamics of nitrate and phosphate in binary systems on a novel adsorbent derived from corn stalks*, J. Geochem. Explor. 188 (2018), pp. 95–100. doi:10.1016/j.gexplo.2018.01.020.

[43] Z. Aksu and F. Gönen, *Biosorption of phenol by immobilized activated sludge in a continuous packed bed: Prediction of breakthrough curves*, Process Biochem. 39 (2004), pp. 599–613. doi:10.1016/S0032-9592(03)00132-8.

[44] J.D. Hem and W.H. Cropper, *Survey of ferrous-ferric chemical equilibria and redox potentials*, 1459-A, U.S. Geological Survey, Washington, U.S., 1959.

[45] K.S. Smith, *Metal sorption on mineral surfaces: An overview with examples relating to mineral deposits*, in *The Environmental Geochemistry of Mineral Deposits, Part A. Processes, Techniques, and Health Issues: Society of Economic Geologists*, Reviews in Economic Geology, 1999, pp. 161–182.

[46] S. Hashemian, S.H. Hosseini, H. Salehifar and K. Salari, *Adsorption of Fe(III) from aqueous solution by Linde type-A zeolite*, Am. J. Anal. Chem. 4 (2013), pp. 123–126. doi:10.4236/ajac.2013.47A017.

APPENDIX A: TAYLOR & FRANCIS THESIS REUSE REQUEST

Taylor & Francis is pleased to offer reuses of its content for a thesis or dissertation free of charge contingent on resubmission of permission request if work is published commercially.

APPENDIX B: OFFICE OF SURFACE MINING, RECLAMATION AND ENFORCEMENT FINAL TECHNICAL REPORT

Additional information about this project and related work can be found in a Final Technical Report for the Office of Surface Mining, Reclamation and Enforcement, entitled: *Development of a Modular Passive Treatment System and Evaluation of Reactive Substrates for Reducing Seasonal Effects of Acid Rock Drainage: Potential Application of Nanoparticles, Chelators, and Low Isoelectric Point Substrates*. This report is included as supplemental material to this thesis, and can also be found at the following link: https://www.osmre.gov/programs/tdt/appliedscience/projects.shtm